

https://dspace.org/

Nonstandard finite difference schemes for some epidemic optimal control problems

Arsene Ouemba Tasse; VUYISWA KUBALASA; B Tsanou; Mbaro-Saman Lubuma

https://hdl.handle.net/10539/45634
WOS

Downloaded from a DSpace repository. https://dspace.org/

Mathematics and Computers in Simulation 228 (2025) 1–22

Contents lists available at ScienceDirect

Mathematics and Computers in Simulation

journal homepage: www.elsevier.com/locate/matcom

Original articles

Nonstandard finite difference schemes for some epidemic optimal control problems

Arsène J. Ouemba Tassé [a,c], Vuyiswa B. Kubalasa [a], Berge Tsanou [b,c], Jean M.-S, Lubuma [a,*]

[a] School of Computer Science and Applied Mathematics, University of the Witwatersrand, Johannesburg, South Africa
[b] Department of Mathematics and Applied Mathematics, University of Pretoria, Pretoria, South Africa
[c] Department of Mathematics and Computer Sciences, University of Dschang, Dschang, Cameroon

ARTICLE INFO

This paper is dedicated to the memory of Professor Jean Meinguet (15 March, 1930 to 15 September, 2023), an outstanding scholar, mentor and teacher of Numerical Analysis and Applied Mathematics, who passed away peacefully in Belgium.

Keywords:
Nonstandard finite difference schemes
Dynamic consistency
Forward backward sweep method
Optimal control
Measles
Ebola
Exit screening
Vaccination
Global stability

ABSTRACT

We construct and analyse nonstandard finite difference (NSFD) schemes for two epidemic optimal control problems. Firstly, we consider the well-known MSEIR system that can be used to model childhood diseases such as the measles, with the vaccination as a control intervention. The second optimal control problem is related to the 2014–2016 West Africa Ebola Virus Disease (EVD) outbreak, that came with the unprecedented challenge of the disease spreading simultaneously in three different countries, namely Guinea, Liberia and Sierra Leone, where it was difficult to control the considerable migrations and travels of people inbound and outbound. We develop an extended SEIRD metapopulation model modified by the addition of compartments of quarantined and isolated individuals. The control parameters are the exit screening of travelers and the vaccination of the susceptible individuals. For the two optimal control problems, we provide the results on: (i) the (global) stability of the disease-free and/or endemic equilibria of the state variable systems; (ii) the positivity and boundedness of solutions of the state variables systems; (iii) the existence, uniqueness and characterization of the optimal control solutions that minimizes the cost functional. On the other hand: (iv) we design Euler-based nonstandard finite difference versions of the Forward-Backward Sweep Method (NSFD-FBSM) that are dynamically consistent with the state variable systems; (v) we provide numerical simulations that support the theory and show the superiority of the nonstandard approach over the classical FBSM. The numerical simulations suggest that significantly increasing the coverage of the vaccine with its implementation for adults as well is essential if the recurrence of measles outbreaks is to be stopped in South Africa. They also show that the optimal control vaccination for the 2014-2016 EVD is more efficient than the exit screening intervention.

1. Introduction

Dynamical systems defined by systems of ordinary differential equations play a vital role in the modelling of real-life problems that arise in a variety of fields in Science, Engineering and Technology (SET). However, most of the differential equation models cannot be completely solved by analytic techniques. Consequently, numerical schemes and simulations are of fundamental importance in gaining some useful insights on the solutions of the differential equations.

* Corresponding author.
E-mail address: jean.lubuma@wits.ac.za (J.M.-S. Lubuma).

https://doi.org/10.1016/j.matcom.2024.08.028
Received 24 January 2024; Received in revised form 5 August 2024; Accepted 23 August 2024
Available online 26 August 2024
0378-4754/© 2024 The Author(s). Published by Elsevier B.V. on behalf of International Association for Mathematics and Computers in Simulation (IMACS). This is an open access article under the CC BY license (http://creativecommons.org/licenses/by/4.0/).

The nonstandard finite difference (NSFD) method was initiated by R.E. Mickens more than three decades ago. In the first two papers [1,2], the founder of the NSFD method made an important observation, namely that the traditional procedures in the design of finite difference schemes had to be suitably changed if the schemes are required to have zero local truncation errors or not to contain instabilities and chaotic behaviour.

The 1994 monograph [3], recently revised and enlarged as [4], constitutes a self-contained and comprehensive treatment of the nonstandard approach. Since its publication, the NSFD method has extensively been applied to differential equation models originating from problems in SET and shown great potential in replicating the dynamics and significant properties of the involved continuous models (see, for instance, the papers [5–9], the books [3,10], the edited volumes [4,11,12] and the review paper [13]).

To the authors' best knowledge, the nonstandard approach has not been used yet for optimal control problems despite its success and the progress made so far. The aim of the current paper is to fill this gap. We construct and analyse NSFD schemes for two epidemic optimal control problems. While the first optimal problem is related to the well-known MSEIR (Infants with temporary passive immunity, Susceptible, Exposed, Infectious, Recovered) model [14,15] with the vaccination as a control parameter, the second optimal control problem, which is related to the 2014–2016 West Africa Ebola Virus Disease (EVD), requires prior construction of a suitable model for the associated state variable system. In this regard, the unprecedented challenge to be factored into the model is that the 2014–2016 EVD simultaneously erupted in three different countries, namely Guinea, Liberia and Sierra Leone [16], where it was difficult to control the considerable migrations and travels of people inbound and outbound [17–20]. We therefore develop an extended SEIRD (Susceptible, Exposed, Infectious, Recovered, Deaths due EVD) metapopulation model, which is enriched by the Q and P compartments of quarantined and isolated individuals, respectively. In this new SEIDQPR model, as the state variable system, we introduce the exit screening of travellers and the vaccination of susceptible individuals as control parameters, thereby defining our second epidemic optimal control problem.

For the two epidemic optimal control problems, we study the existence, the uniqueness and the characterization of the optimal control solutions that minimize the cost functional by using, among other tools, Pontryagin maximum principle. Furthermore, we design Euler-based NSFD-Forward Backward Sweep Methods (NSFD-FBSM) that preserve the dynamics of the state variable systems and generate numerical simulations that support the theory and illustrate the superiority of the NSFD-FBSM over the classical FBSM. Since our main focus is to construct, analyse and implement NSFD schemes for epidemic optimal control problems, we state the results for the underlying continuous models, and provide only clear indications and or references for their proofs.

The rest of the paper is structured as follows. In Section 2, some generalities about the optimal control theory are presented. Section 3 deals with NSFD schemes in the general context. In Section 4, we study theoretically and numerically (NSFD-FBSM) of the optimal control MSEIR problem with vaccination as a control. The same thing is done in Section 5, but for an EVD metapopulation model with exit screening and vaccination control measures. Concluding remarks and the discussion are given in Section 6.

2. About optimal control problems

The theoretical setting of this paper is an optimal control problem [21]

$$J(x^*, u^*) = \min_{u \in U} J(x, u) \tag{1}$$

subject to

$$\begin{cases} \dfrac{dx}{dt}(t) = g(t, x(t), u(t)) \\ x(0) = x_0, \end{cases} \tag{2}$$

where:

- $$U := \{u : [0,T] \to \mathbb{R}^m, \text{ Lebesgue measurable}\}$$
  is the set of admissible controls;
- Eq. (2) is supposed to be a dynamical system on an attractive compact set $\Omega \subset \mathbb{R}^n$, for $u(t)$ constant, with the function $g : [0,T] \times \Omega \times U \to \mathbb{R}^n$ being continuous in its three arguments;
- With, $f : [0,T] \times \Omega \times U \to \mathbb{R}$ a continuous function in its three arguments, J is the objective or cost functional defined by
  $$J(x,u) := \int_0^T f(t, x(t), u(t))dt.$$

Further conditions and/or smoothness properties on the functions involved in (1)–(2) will be stated where they are needed. In Eqs. (1), u^* is called an optimal control in the set U, while x^* is an associated solution of the state Eq. (2). The pair (u^*, x^*) is an optimal solution of the optimal control problem (1)–(2).

To reformulate the constrained problem (1)–(2) as a problem without constraints, we introduce a new variable $\lambda : [0,T] \to \mathbb{R}^n$, the adjoint variable, through the Hamiltonian, $H \equiv H(t, x(t), u(t), \lambda(t))$, of the optimal control problem (1)–(2), defined by

$$H(t, x(t), u(t), \lambda(t)) = f(t, x(t), u(t)) + \langle \lambda(t) \mid g(t, x(t), u(t)) \rangle, \tag{3}$$

where $\langle . \mid . \rangle$ denotes the inner product in $\mathbb{R}^n$. The necessary conditions for the existence of an optimal control solution is the Pontryagin maximum principle that, in the context of this paper, is stated for a minimization problem as follows [22]:

Theorem 1. *If the pair (u^*, x^*) is an optimal solution of Problem (1)–(2), then there exists a piecewise continuously differentiable adjoint variable $\lambda : [0,T] \to \mathbb{R}^n$ such that the following statements hold:*

- *Optimality conditions:*

$$H(t, x^*(t), u^*(t), \lambda(t)) \leq H(t, x^*(t), u(t), \lambda(t)) \tag{4}$$

for any control $u \in U$ and at every time $t \in [0,T]$. This implies that $\frac{\partial H}{\partial u_i} = 0$.

- *Adjoint or costate system: λ solves the adjoint system*

$$\frac{d\lambda}{dt} = -\frac{\partial H(t, x^*(t), u^*(t), \lambda(t))}{\partial x_i}, \ i = 1, 2, \dots, n. \tag{5}$$

- *Transversality condition:*

$$\lambda(T) = 0. \tag{6}$$

In epidemiology of human infectious diseases, which is our primary interest, the optimal control problems are such that the controls are nonnegative and bounded. We therefore assume that a control $u \in U$ is such that

$$\text{for almost every } t \in [0,1],\ 0 \leq u_i(t) \leq 1,\ i = 1, \dots, m, \ \text{or } u(t) \in [0,1]^m. \tag{7}$$

Furthermore, we impose additional conditions on the involved functions so that the Pontryagin's necessary conditions in Theorem 1 become sufficient for the existence of an optimal control solution to (1)–(2), which is possibly unique. For simplicity and in light of the epidemic optimal control problems under consideration in this work, we state the result for scalar controls i.e. $m = 1$ [22], though extensions to vector-valued controls are available (see, for instance, the Arrow sufficient theorem in [23]).

Theorem 2.

1. *Assume that the function $f(t,x,u)$ is convex in the argument u. Further, assume that this function and the function $g(t,x,u)$ have the following behaviour for all $t \in [0,T], x \in \mathbb{R}^n$ and $u \in \mathbb{R}$*

$$\begin{aligned} &g(t,x,u) \leq \alpha(t,x) + \beta(t,x)u \\ &|g(t,x,u)| \leq C(1 + |x| + |u|) \\ &|g(t,x,u) - g(t,\widetilde{x},u)| \leq C|x - \widetilde{x}|(1 + |u|) \\ &f(t,x,u) \geq C|u|^\gamma - C \end{aligned} \tag{8}$$

   where $\alpha, \beta : [0,T] \times \mathbb{R}^n \to \mathbb{R}^n$, $\gamma \geq 1$, and $C > 0$ represents a generic constant that is different in each occurrence and is independent of the arguments. Then, there exists an optimal control solution (u^*, x^*) of (1)–(2) with $J(x^*, u^*)$ finite.
2. *In the particular case where the functions f and g as well as the right-hand side of the system (5) are Lipschitz on the state and costate variables, the solution of the optimality system (1), (2), (4) and (5) is unique for small time.*
3. *Finally, assume that the controls are bounded as in (7), i.e., $0 \leq u(t) \leq 1$. Then, the optimal control u^* is given by*

$$u^*(t) = \begin{cases} 1 & \text{if } 0 \leq t \leq T^* \\ 0 \leq u^* \leq 1 & \text{if } T^* \leq t \leq T^{**} \\ 0 & \text{if } T^{**} < t \leq T \end{cases} \tag{9}$$

   and thus,

$$u^* = \min\left\{1, \max\{0, \{u : \frac{\partial H}{\partial u} = 0\}\right\} \quad \text{or} \quad u^* = \max\left\{0, \min\{1, \{u : \frac{\partial H}{\partial u} = 0\}\right\}, \tag{10}$$

   where T^* is the largest time in the interval $[0,T]$ such that $\frac{\partial H}{\partial u} < 0$, while T^{**} is the smallest time in $[T^*, T]$ such that $\frac{\partial H}{\partial u} > 0$.

3. Nonstandard finite difference forward backward sweep method

It is well-known that classical numerical methods such as the Euler, the explicit Runge Kutta and linear multistep methods generally fail to preserve the dynamics of the differential equation models. For instance, these schemes can exhibit spurious/ghost solutions, a phenomenon reported as elementary instability [3,7]. The nonstandard finite difference (NSFD) method introduced by Mickens [3] more than three decades ago has shown great potential and is increasingly being used in various areas of Sciences, Engineering and Technology (SET) to produce dynamically consistent schemes [3,6,7,9,10]. In this section, we propose NSFD schemes to solve optimal control problems, using the forward backward sweep method (FBSM) [22]. We will focus on Euler-based NSFD schemes, thereby rehabilitating the classical forward and backward Euler schemes, which have the advantage of being simple to implement. We start with the dynamical system on Ω defined by the state variable System (2) where we assume for the moment, that there is no control i.e., $u(t) \equiv 0$ and thus

$$g(t, x(t)) \equiv g(t, x(t), 0). \tag{11}$$

Given an integer $p > 1$, we divide the interval $[0, T]$ into p subintervals $[t_i, t_{i+1}]$ of equal size $\Delta t = T/p$ where $t_i = i\Delta t$, $i = 0, 1, \dots, p-1$. We denote by $x_i = (x_{1i}, x_{2i}, \dots, x_{ni})$ an approximation of the solution $x(t) \equiv (x_1(t), x_2(t), \dots, x_n(t))$ of (2)&(12) at the time $t = t_i$:

$$x_i \simeq x(t_i) \tag{12}$$

The NSFD forward Euler scheme that we will use is based on Mickens rule, (Rule 2 [7]), of the nontrivial denominator function of the discrete derivative, instead of the step size Δt. It reads as follows: for $i = 0, 1, 2, \dots, p-1$,

$$\frac{x_{i+1} - x_i}{r(\Delta t)} = g(t_i, x_i),\ x_0 = x(0) \tag{13}$$

where, with $q > 0$ to be determined in due course,

$$r \equiv r = \frac{1 - e^{-q\Delta t}}{q} = \Delta t + \mathcal{O}(\Delta t^2) \tag{14}$$

For epidemic models, the state system (2) &(12) with respect to which the set $\mathbb{R}^n_+$ is forward invariant will have the so-called productive-destructive form [9], namely

$$g(t, x) = b(x) - x \otimes d(x), \tag{15}$$

where the two vector functions satisfy $b(x) \geq 0$, $d(x) \geq 0$ for $x \geq 0$, and the symbols $\otimes$ represents the tensor product of two vectors. In this case, we will construct NSFD schemes by both Rule 2 above and Mickens' Rule 3 on the nonlocal discretization of nonlinear terms as follows: for $i = 0, 1, 2, \dots, p-1$,

$$\frac{x_{i+1} - x_i}{r} = b(x_i) - x_{i+1} \otimes d(x_i), \quad x_0 = x(0). \tag{16}$$

Remark 3. The asymptotic behaviour of $r(\Delta t)$ in (14) guarantees that the NSFD schemes are convergent and the rate of convergence is 1 as for the classical Euler scheme. The key point is that the dynamics of the continuous model must be properly incorporated into the definition of the function $r(\Delta t)$. In a nutshell, by choosing the parameter q such that it captures the dynamics of the system (2), we will show later, for epidemic models that the NSFD schemes (13) and/or (16) are discrete dynamical systems on Ω that preserve the properties of the continuous system such as the equilibrium and their stability properties as well as the positivity and boundedness of solutions.

We now turn to the construction of a reliable numerical method for the initial value state system (2) and the adjoint system (5) coupled with the transversality condition (6) which, for convenience, are rewritten as follows:

$$\begin{cases} x'(t) = g(t, x(t), u(t)), & x(0) = x_0 \\ \lambda'(t) = \varphi(t, x(t), \lambda(t), u(t)), & \lambda(T) = 0 \\ u(t) = h(t, x(t), \lambda(t)) \end{cases} \tag{17}$$

where $\varphi(t, x(t), \lambda(t), u(t)) = -(f_x(t, x(t), u(t)) + \langle \lambda(t) \mid g_x(t, x(t), u(t))\rangle)$, and the function h defining u comes from (9)–(10).

The discretization of the interval $[0, T]$ through nodes (t_i) was done earlier. The notation u_i and λ_i have the same meaning as x_i in (12). For iterations $m \geq 0$ and choosing an initial guess $u^{(0)} = u^{(0)}(t)$, the continuous Forward Backward Sweep Method (FBSM) aims to find, at each iteration, $x^{(m+1)}$, $\lambda^{(m+1)}$ and $u^{(m+1)}$, solutions of the following systems:

$$\begin{cases} \dfrac{dx^{(m+1)}(t)}{dt} = g(t, x^{(m+1)}(t), u^{(m)}(t)), & x^{(m+1)}(0) = x_0 \\ \dfrac{d\lambda^{(m+1)}(t)}{dt} = \varphi(t, x^{(m+1)}(t), \lambda^{(m+1)}(t), u^{(m)}(t)), & \lambda^{(m+1)}(T) = 0 \\ u^{(m+1)}(t) = h(t, x^{(m+1)}(t), \lambda^{(m+1)}(t)). \end{cases} \tag{18}$$

The algorithm to approximate the system in (18) is described in the four steps below.

1. For $m = 0$, choose an initial guess $u_i^{(0)}$ for $i = 0, \dots, p$;
2. For $m \geq 0$:
   - Compute $x_{i+1}^{(m+1)}$ by the nonstandard forward Euler scheme (13) as follows:

$$\frac{x_{i+1}^{(m+1)} - x_i^{(m+1)}}{r} = g(t, x_i^{(m+1)}, u_i^{(m)}),\ \ x_{0,i}^{(m+1)}(0) = x_{0,i}$$

or, equivalently,

$$x_{i+1}^{(m+1)} = x_i^{(m+1)} + rg(t, x_i^{(m+1)}, u_i^{(m)}) \text{ for } i = 0, 1, \dots, p-1, \tag{19}$$

   where the denominator function r is defined as in (14) such that the following minimum requirement on q for the stability of equilibrium points holds:

$$q > \left\{ \frac{|\sigma|}{(2|\Re e\sigma|)} \right\}, \tag{20}$$

where σ runs in the set of all eigenvalues of the Jacobian matrices of the right-hand side of System (2) evaluated at the equilibria [6].

- Compute $\lambda_i^{(m+1)}$ by the classical backward Euler scheme as follows:

$$\frac{\lambda_{i+1}^{(m+1)} - \lambda_i^{(m+1)}}{\Delta t} = \varphi(t_{i+1}, x_{i+1}^{m+1}, \lambda_{i+1}^{m+1}, u_i^m), \quad \lambda_p^{(m+1)} = 0$$

or, equivalently,

$$\lambda_i^{(m+1)} = \lambda_{i+1}^{(m+1)} - \Delta t \varphi(t_{i+1}, x_{i+1}^{m+1}, \lambda_{i+1}^{m+1}, u_i^m) \text{ for } i = p-1, \dots, 0.$$

3. Update the discrete control as follows:

$$u_{i+1}^{(m+1)} = h(t_{i+1}, x_{i+1}^{(m+1)}, \lambda_{i+1}^{(m+1)}) \text{ for } i = 0, 1, \dots, p.$$

4. We stop the process at the iteration m once the values of the unknowns at the previous iteration are very close to the ones at the present iteration [22]. Otherwise, we repeat the process in the loop from item 2 with the iteration $m+1$.

Remark 4. It can be difficult to numerically solve the system (18) since it is a two-point boundary value problem. This explains why, for each loop of the algorithm, the strategy is that the state variable system is solved forward in time from 0 to T, while the adjoint equation is solved backward in time from T to 0. The proof of the convergence of the FBSM can be found in [24].

In the following sections, we construct Euler-based NSFD-FBSM for epidemic control problems and show the superiority of these new schemes over the classical FBSM.

4. The MSEIR model

4.1. Optimal control

The first epidemic model we consider is the MSEIR system [14]. Though this system is well-known to model childhood diseases [25], we specifically use it to get insight on the optimal control and eradication of the measles disease in light of the October 2022 – April 2023 outbreak in South Africa [26]. However, we use here a relatively simple version of the MSEIR model proposed in [15], as the MSIR to which we add the latent compartment. More precisely, we divide the total population, $N \equiv N(t)$ at time t, into five mutually exclusive compartments: $M := M(t)$, the compartment of infants with temporary passive immunity transferred from their mothers at birth; $S := S(t)$, the compartment of individuals who are susceptible to the measles virus; $E := E(t)$, the compartment of individuals exposed to the measles virus; $I := I(t)$, the compartment of infectious individuals and $R := R(t)$, the compartment of recovered individuals. The description of model parameters are provided on Table 1, respectively. The model is given by the system of ordinary differential equations below.

$$\begin{cases} \frac{dM}{dt} &= (1-b)\Lambda - (d+\delta)M \\ \frac{dS}{dt} &= b\Lambda - \beta\frac{SI}{N} - dS + \delta M \\ \frac{dE}{dt} &= \beta\frac{SI}{N} - (\epsilon + d)E \\ \frac{dI}{dt} &= \epsilon E - (\gamma + d + \alpha)I \\ \frac{dR}{dt} &= \gamma I - dR. \end{cases} \tag{21}$$

The system is subject to the non-negative initial conditions

$$M(0) = M_0,\ S(0) = S_0,\ E(0) = E_0,\ I(0) = I_0,\ R(0) = R_0. \tag{22}$$

It is biologically sound to assume that the effective transmission number is greater than the infective death rate: $\beta > \alpha$. It is clear that the first equation in (21) has, for $M_0 \geq 0$, a unique solution

$$M(t) = \frac{(1-b)}{d+\delta}\Lambda + M_0 e^{-(d+\delta)t}, \quad \forall\, t > 0, \tag{23}$$

and a unique equilibrium point

$$M^* = \frac{(1-b)\Lambda}{d+\delta},$$

which is globally asymptotically stable. Injecting the solution of Eq. (23) into the other equations of Model (21), we obtain the following result:

Table 1
Description of parameters used in the model.

Parameters	Parameter description	Units	Values	Ref
b	Fraction of infants without immunity	–	0.39	[15]
d	Natural death rate	day^{-1}	0.01143/365	Estimated
$1/\alpha$	Time from the infection to death	day^{-1}	1/58	Assumed
β	Effective contact number	day^{-1}	60	Assumed
δ	Loss of immunity rate	day^{-1}	1/180	[14]
$1/\epsilon$	Duration of the latent period	day^{-1}	1	Assumed
γ	Recovery rate	day^{-1}	0.47	[15]
Λ	Recruitment constant	individual/day	1879	Estimated

Theorem 5.

1. *The MSEIR Model (21) is a dynamical system on the biologically feasible region*

$$\Omega = \left\{ (M, S, I, E, R) \in \mathbb{R}^5_+ : 0 \le N \le \frac{\Lambda}{d} \right\},$$

which attracts all solutions starting outside Ω.

2. *The model always admits a unique disease-free equilibrium E^* given as*

$$E^* = (M^*, S^*, E^*, I^*, R^*) = \left(\frac{(1-b)\Lambda}{d+\delta}, \frac{\Lambda(bd+\delta)}{d(d+\delta)}, 0, 0, 0 \right) \tag{24}$$

3. *The basic reproduction number of Model (21) is given as*

$$\mathcal{R}_0 = \frac{\beta\epsilon(bd+\delta)}{(d+\epsilon)(d+\delta)(\gamma+d+\alpha)}.$$

4. *The disease-free equilibrium is locally asymptotically stable (LAS) whenever $\mathcal{R}_0 < 1$. It is unstable when $\mathcal{R}_0 > 1$.*
5. *When $\mathcal{R}_0 > 1$, the Model (21) admits a unique endemic equilibrium $E^{**} := (M^{**}, S^{**}, E^{**}, I^{**}, R^{**})$, with*

$$\begin{cases} M^{**} = \dfrac{(1-b)\Lambda}{d+\delta}, & S^{**} = \dfrac{\Lambda(bd+\delta)}{d(d+\delta)(\beta-\alpha)}\left(\dfrac{\beta}{\mathcal{R}_0} - \alpha\right) \\ E^{**} = \dfrac{\Lambda(\gamma+d+\delta)}{(\beta-\alpha)\epsilon}(\mathcal{R}_0 - 1), & I^{**} = \dfrac{\Lambda}{(\beta-\alpha)}(\mathcal{R}_0 - 1), \\ R^{**} = \dfrac{\gamma\Lambda}{d(\beta-\alpha)}(\mathcal{R}_0 - 1). \end{cases} \tag{25}$$

In this case, the endemic equilibrium is GAS.

The results in 5 can be obtained as for the variants models of (21) investigated in [14,15]. Note that statements in items (4) and (5) of Theorem 5 are a rephrasing of the fact that the MSEIR model (21) enjoys the sharp threshold property introduced in [27]. In this reference, Lyapunov functions are constructed in a systematic manner and they are used to establish the global asymptotical stability of the disease-free equilibrium and the endemic equilibrium when $\mathcal{R}_0 \le 1$ and $\mathcal{R}_0 > 1$, respectively.

As alluded to earlier, childhood diseases such as Measles, Mumps and Rubella (MMR) can be modelled by the MSEIR system. We now want to introduce the vaccination as a control intervention in the MSEIR model. We assume that at the time t, the susceptible infants are vaccinated at the t-dependent rate $u(t)$. Given that the MMR vaccine is 99% effective after two doses [28], we assume for the sake of simplicity of our model that vaccine is 100% effective. This leads to the system

$$\begin{cases} M' = (1-b)\Lambda - (\delta+d)M, & M(0) = M_0 \ge 0 \\ S' = b\Lambda + \delta M - \beta\dfrac{SI}{N} - dS - uS, & S(0) = S_0 \ge 0 \\ E' = \beta\dfrac{SI}{N} - (d+\epsilon)E, & E(0) = E_0 \ge 0 \\ I' = \epsilon E - (\gamma+d+\alpha)I, & I(0) = I_0 \ge 0 \\ R' = \gamma I - dR + uS, & R(0) = R_0 \ge 0 \end{cases} \tag{26}$$

which can be written in the compact form (2) as

$$x' = g(t, x(t), u(t)), \tag{27}$$

where $x = (M(t), S(t), E(t), I(t), R(t))$, $x_0 = (M_0, S_0, E_0, I_0, R_0)$ and $g(t, x(t), u(t))$ is defined by the right hand side of (26).

Our goal is to minimize the following cost functional defined, as in [22], by

$$J(x, u) = \int_0^T AI(t) + u(t)^2 dt, \quad i.e., \quad f(t, x, u) = AI(t) + u^2(t) \text{ in (18).} \tag{28}$$

Here $A \ge 0$ is the weight parameter linked to the variable I and the function u belongs to the set

$$U = \{v,\ v \text{ Lebesgue measurable},\ 0 \le v(t) \le 0.8, \text{ for almost every } t \in [0, T]\}. \tag{29}$$

Similar to [22], the upper bound of the controls is set to much less than 1 in (29) because it is impossible to vaccinate all the population. The specific upper bound 0.8 is chosen, due to the reported low coverage of the MMR vaccine in South Africa, the country under consideration for this study [26,29].

By adding the equations in (26), we have the conservation law

$$\frac{dN}{dt} = \Lambda - dN - \alpha I.$$

Thus, the state variable, $(\bar{M}, \bar{S}, \bar{E}, \bar{I}, \bar{R})$, of an optimal solution of the optimal control problem belongs to the biologically feasible region Ω. More so, we have the following straightforward result.

Theorem 6. *For $u(t) = constant$, the dynamical System (26) enjoys qualitative properties similar to those in Theorem 5.*

It can be shown that the above specified functions $g(t,x,u)$ and $f(t,x,u)$ satisfy the assumptions stated in Theorem 2. For instance, in the expressions of the C^1 functions f and g in Eqs. (26), (27) and (28), it is clear that f is convex, while the first and the third inequalities of Condition (8) is obvious. Regarding the second condition, we have

$$\begin{aligned}
\| g(t,x,u) \|^2 &= [(1-b)\Lambda - (\delta+d)M]^2 + [b\Lambda + \delta M - \tfrac{\beta IS}{N} - (d+u)S]^2 + [\tfrac{\beta IS}{N} - (d+\epsilon)E]^2 \\
&\quad [\epsilon E - (\gamma+d+\alpha)I]^2 + [\gamma I - dR + uR]^2 \\
&\leq (1-b)^2\Lambda^2 + (\delta+d)^2M^2 + (b\Lambda+\delta M)^2 + 2\beta^2S^2 + (d+u)^2S^2 + 2\beta(d+u)S \\
&\quad + ((d+\epsilon)^2+\epsilon^2)E^2 + I^2[(\gamma+d+\alpha)^2+\gamma^2] + u^2S^2 + 2\gamma u\tfrac{\Lambda^2}{d^2} + d^2R^2 \\
&\leq M^2((\delta+d)^2+\delta^2) + S^2(2\beta^2+d^2) + ((d+\epsilon)^2+\epsilon^2)E^2 \\
&\quad + ((\gamma+d+\alpha)^2+\gamma^2)I^2 + d^2R^2 + u^2(\tfrac{2\Lambda^2}{d^2}) + \tfrac{2b\Lambda^2\delta}{d} \\
&\quad + b^2\Lambda^2 + 2d + 2\beta(d+1)\tfrac{\Lambda}{d} + \tfrac{2\gamma\Lambda^2}{d^2} \\
&\leq C(1+\| x \| + |u|)^2
\end{aligned}$$

where

$$\begin{aligned}
C &= \max\{\tfrac{2b\Lambda^2\delta}{d} + b^2\Lambda^2 + 2d + 2\beta(d+1)\tfrac{\Lambda}{d} + \tfrac{2\gamma\Lambda^2}{d^2}; (\delta+d)^2+\delta^2; 2\beta^2+d^2; \\
&\quad (d+\epsilon)^2+\epsilon^2; (\gamma+d+\alpha)^2+\gamma^2; d^2; \tfrac{2\Lambda^2}{d^2}\}.
\end{aligned}$$

Consequently, with additionally Theorem 1, we have the following existence and characterization result for the optimal control problem under consideration.

Theorem 7. *System (26) admits a unique control $u^* \in U$ and an associated trajectory x_u^* such that the objective functional J is minimized. The Hamiltonian of System (26) being*

$$\begin{aligned}
H(t,x,u,\lambda) &= AI(t) + u(t)^2 + \lambda_1\left((1-b)\Lambda - (\delta+d)M\right) + \lambda_2\left(b\Lambda + \delta M - \beta\frac{SI}{N} - dS - u(t)S\right) \\
&+ \lambda_3\left(\beta\frac{SI}{N} - (d+\epsilon)E\right) + \lambda_4\left(\epsilon E - (\gamma+d+\alpha)I\right) + \lambda_5\left(\gamma I - dR + u(t)S\right),
\end{aligned} \tag{30}$$

an optimal control solution (u^*, x^*) is characterized as follows in three steps:

- *The function $\lambda := (\lambda_1, \lambda_2, \lambda_3, \lambda_4, \lambda_5)$ is the solution of the adjoint system [30]*

$$\begin{cases}
\lambda_1' &= -\dfrac{\partial H}{\partial M} = -\lambda_1(\delta+d) + \lambda_2\left(\delta + \beta\dfrac{SI}{N^2}\right) - \lambda_3\beta\dfrac{SI}{N^2} \\
\lambda_2' &= -\dfrac{\partial H}{\partial S} = -\lambda_2\left(-d - u(t) + \beta\dfrac{I(M+E+I+R)}{N^2}\right) - \lambda_3\beta\dfrac{I(M+E+I+R)}{N^2} - \lambda_5 u(t) \\
\lambda_3' &= -\dfrac{\partial H}{\partial E} = -\lambda_2\beta\dfrac{SI}{N^2} - \lambda_3\left(-\beta\dfrac{SI}{N^2} - (d+\epsilon)\right) - \lambda_4\epsilon \\
\lambda_4' &= -\dfrac{\partial H}{\partial I} = -A - \lambda_2\beta\dfrac{I(M+S+E+R)}{N^2} - \lambda_3\beta\dfrac{I(M+S+E+R)}{N^2} + \lambda_4(\gamma+d+\alpha) - \lambda_5\gamma \\
\lambda_5' &= -\dfrac{\partial H}{\partial R} = -\lambda_2\beta\dfrac{SI}{N^2} + \lambda_3\beta\dfrac{SI}{N^2} + \lambda_5 d
\end{cases}$$

  subject to the transversality conditions

$$\lambda_1(T) = \lambda_2(T) = \lambda_3(T) = \lambda_4(T) = \lambda_5(T) = 0.$$

- *The control u^* is a critical point of H, i.e.,*

$$0 = \frac{\partial H}{\partial u} = 2u(t) - \lambda_2(t)S(t) + \lambda_5(t)S(t) \text{ at } u^*. \tag{31}$$

- *The optimal control is*

$$u^*(t) \equiv \begin{cases} 0 & \text{for } 0 \leq t < T^* \\ \dfrac{1}{2}(\lambda_2 - \lambda_5)S & \text{for } T^* \leq t \leq T^{**} \\ 0.8 & \text{for } T^{**} < t \leq T \end{cases} \tag{32}$$

where T^* is the largest time in the interval $[0,T]$ such that $\frac{\partial H}{\partial u} > 0$ at $u = 0$ and T^{**} is the smallest time in the interval $[T^*,T]$ such that $\frac{\partial H}{\partial u} < 0$ at $u = 0.8$.

With the material accumulated till now, we are in a position to design an Euler-based nonstandard finite difference forward backward sweep method (NSFD-FBSM) from the continuous FBSM below. For $m = 0,1,2,\ldots$ and given $u^{(m)}$ solve:

$$\begin{cases} \dfrac{dx^{(m+1)}}{dt} = g(t,x^{(m+1)},u^{(m)}),\ x^{(m+1)}(0) = x_0 \\ \dfrac{d\lambda^{(m+1)}}{dt} = \varphi(t,x^{(m+1)},\lambda^{(m+1)},u^{(m)}),\ \lambda^{(m+1)}(T) = 0 \\ u^{(m+1)} = \dfrac{1}{2}(\lambda_2^{(m+1)} - \lambda_5^{(m+1)})S^{(m+1)} \equiv h(t,x^{(m+1)},\lambda^{(m+1)}) \end{cases} \tag{33}$$

where the state variable system has the productive-destructive form (15), as seen in (26). The Euler-based NSFD-FBSM for the system (33) consists of the steps below.

- For $m = 0$, choose an initial guess $u_j^{(0)}$, for $j = 0,1,\ldots,p$.
- For $m \geq 0$:
  - Compute $(M_{j+1}^{(m+1)}, S_{j+1}^{(m+1)}, E_{j+1}^{(m+1)}, I_{j+1}^{(m+1)}, R_{j+1}^{(m+1)})$ by the NSFD scheme (14) and (16) explicitly detailed, in the Gauss–Seidel order, as follows: for $j = 0,1,\ldots,p$ and with $(M_0^{(m+1)}, S_0^{(m+1)}, E_0^{(m+1)}, I_0^{(m+1)}, R_0^{(m+1)}) = (M_0,S_0,E_0,I_0,R_0) \geq 0$,

$$\begin{cases} \dfrac{M_{j+1}^{(m+1)} - M_j^{(m+1)}}{r} &= (1-b)\Lambda - (\delta+d)M_{j+1}^{(m+1)} \\ \dfrac{S_{j+1}^{(m+1)} - S_j^{(m+1)}}{r} &= b\Lambda + \delta M_{j+1}^{(m+1)} - \beta\dfrac{S_{j+1}^{(m+1)} I_j^{(m+1)}}{N_j^{(m+1)}} \\ & \quad - dS_{j+1}^{(m+1)} - u_j^{(m)} S_{j+1}^{(m+1)} \\ \dfrac{E_{j+1}^{(m+1)} - E_j^{(m+1)}}{r} &= \beta\dfrac{S_{j+1}^{(m+1)} I_j^{(m+1)}}{N_j^{(m+1)}} - (d+\epsilon)E_{j+1}^{(m+1)} \\ \dfrac{I_{j+1}^{(m+1)} - I_j^{(m+1)}}{r} &= \epsilon E_{j+1}^{(m+1)} - (\gamma+d+\alpha)I_{j+1}^{(m+1)} \\ \dfrac{R_{j+1}^{(m+1)} - R_j^{(m+1)}}{r} &= \gamma I_{j+1}^{(m+1)} - dR_{j+1}^{(m+1)} + u_j^{(m)} S_{j+1}^{(m+1)} \end{cases} \tag{34}$$

    where r is defined in (14), with $q \geq d+\delta+\alpha+\epsilon+\gamma$ satisfying (20).
  - Compute $\lambda_j^{(m+1)}$ with $\lambda_p^{(m+1)} = 0$ by the classical backward Euler scheme: for $j = p-1, p-2, \ldots, 0$.

$$\begin{cases} \dfrac{\lambda_{1j+1}^{(m+1)} - \lambda_{1j}^{(m+1)}}{\Delta t} &= -\lambda_{1j+1}^{(m+1)}(\delta+d) + \lambda_{2j+1}^{(m+1)}\left(\delta + \beta\dfrac{S_{j+1}^{(m+1)} I_{j+1}^{(m+1)}}{(N_{j+1}^{(m+1)})^2}\right) \\ & \quad - \lambda_{3j+1}^{(m+1)}\beta\dfrac{S_{j+1}^{(m+1)} I_{j+1}^{(m+1)}}{(N_{j+1}^{(m+1)})^2} \\ \dfrac{\lambda_{2j+1}^{(m+1)} - \lambda_{2j}^{(m+1)}}{\Delta t} &= -\lambda_{2j+1}^{(m+1)}\left(-d - u_{j+1}^{(m)} + \beta\dfrac{I_{j+1}^{(m+1)}(M_{j+1}^{(m+1)} + E_{j+1}^{(m+1)} + I_{j+1}^{(m+1)} + R_{j+1}^{(m+1)})}{(N_{j+1}^{(m+1)})^2}\right) \\ & \quad - \lambda_{3j+1}^{(m+1)}\beta\dfrac{I_{j+1}^{(m+1)}(M_{j+1}^{(m+1)} + E_{j+1}^{(m+1)} + I_{j+1}^{(m+1)} + R_{j+1}^{(m+1)})}{(N_{j+1}^{(m+1)})^2} - \lambda_{5j+1}^{(m+1)} u_{j+1}^{(m)} \\ \dfrac{\lambda_{3j+1}^{(m+1)} - \lambda_{3j}^{(m+1)}}{\Delta t} &= -\lambda_{2j+1}^{(m+1)}\beta\dfrac{S_{j+1}^{(m+1)} I_{j+1}^{(m+1)}}{(N_{j+1}^{(m+1)})^2} - \lambda_{3j+1}^{m+1}\left(-\beta\dfrac{S_{j+1}^{(m+1)} I_{j+1}^{(m+1)}}{(N_{j+1}^{(m+1)})^2} - (d+\epsilon)\right) \\ & \quad - \lambda_{4j+1}^{(m+1)}\epsilon \\ \dfrac{\lambda_{4j+1}^{(m+1)} - \lambda_{4j}^{(m+1)}}{\Delta t} &= -A - \lambda_{2j+1}^{(m+1)}\beta\dfrac{I_{j+1}^{(m+1)}(M_{j+1}^{(m+1)} + S_{j+1}^{(m+1)} + E_{j+1}^{(m+1)} + R_{j+1}^{(m+1)})}{(N_{j+1}^{(m+1)})^2} \\ & \quad - \lambda_{3j+1}^{(m+1)}\beta\dfrac{I_{j+1}^{(m+1)}(M_{j+1}^{(m+1)} + S_{j+1}^{(m+1)} + E_{j+1}^{(m+1)} + R_{j+1}^{(m+1)})}{(N_{j+1}^{(m+1)})^2} \\ & \quad + \lambda_{4j+1}^{(m+1)}(\gamma+d+\alpha) - \lambda_{5j+1}^{(m+1)}\gamma \\ \dfrac{\lambda_{5j+1}^{(m+1)} - \lambda_{5j}^{(m+1)}}{\Delta t} &= -\lambda_{2j+1}^{(m+1)}\beta\dfrac{S_{j+1}^{(m+1)} I_{j+1}^{(m+1)}}{(N_{j+1}^{(m+1)})^2} + \lambda_{3j+1}^{(m+1)}\beta\dfrac{S_{j+1}^{(m+1)} I_{j+1}^{(m+1)}}{(N_{j+1}^{(m+1)})^2} + \lambda_{5j+1}^{(m+1)} d \end{cases}$$

Table 2
Initial conditions to simulate the optimal control problem (26).

Variables	$M(0)$	$S(0)$	$E(0)$	$I(0)$	$R(0)$
Initial conditions	250,000	20,000,000	5,612[26]	931[26]	500

With $\lambda_{i,j}^{m+1} = 0$, for $j = p$ and $i = 1, 2, 3, 4, 5$, it is easy to check that, for $j = p-1, p-2, \dots, 0$, the following simple and explicit expression holds:

$$\lambda_{4,p-1}^{m+1} = A\Delta t \text{ and } \lambda_{i,j}^{m+1} = \begin{cases} 0 & \text{if } i \neq 4 \\ A\Delta t + (1 - \Delta t(\gamma + d + \alpha))\lambda_{4,p-l+1}^{m+1} & \text{if } i = 4 \text{ and } j = p-l, \\ & l = 1, 2, \dots, p-1. \end{cases} \tag{35}$$

Note that the second bullet of the Euler-based NSFD-FBSM falls in the category of symplectic schemes for optimal control problems (see, for instance, [31] and the references therein).

By adding the equations of System (34), it is clear that the NSFD scheme satisfies the following discrete counterpart of the conservation law:

$$\frac{N_{j+1}^{m+1} - N_j^{m+1}}{r} = \Lambda - dN_{j+1}^{m+1} - \alpha I_{j+1}^{m+1} \leq \Lambda - dN_{j+1}^{m+1}. \tag{36}$$

Hence,

$$N_{j+1}^{m+1} \leq \frac{\Lambda}{d} \text{ whenever } N_j^{m+1} \leq \frac{\Lambda}{d}.$$

This leads to the result.

Theorem 8. *For a constant discrete control, $u_j^m = \tilde{u}$, the NSFD scheme for the state variables preserves the positivity and boundedness of the continuous state variables in the sense that*

$$(M_0^{m+1}, S_0^{m+1}, E_0^{m+1}, I_0^{m+1}, R_0^{m+1}) \in \Omega \implies (M_j^{m+1}, S_j^{m+1}, E_j^{m+1}, I_j^{m+1}, R_j^{m+1}) \in \Omega. \tag{37}$$

4.2. Numerical solutions

NSFD theta (Euler for $\theta = 0$ or $\theta = 1$) schemes for the MSEIR model with constant control (e.g., $u = 0$) are constructed and analysed in [32] where numerical simulations that illustrate the preservation of the stability of the equilibrium points as well as the positivity and boundedness of the solutions, as per Theorem 8, are given. Here, we are interested in the impact of the control. We apply the NSFD-FBSM developed in the previous subsection to solve the optimal control problem (26).

The involved parameters are estimated as explained below, based on the reality of the October 2022 to April 2023 measles outbreak in South Africa [26,29]. From these references, it is reported that laboratory tests performed on a sample of 5612 individuals, resulted in 931 cases. We, therefore, take the initial conditions $E(0) = 5612$ and $I(0) = 931$. Furthermore, it is highlighted in the same references that the coverage of the MMR vaccine is alarmingly below the 95% target that is needed to eradicate the measles disease, while a significant number of adults fail to receive the first dose of the vaccine. This means that the number of individuals, including adults, who are susceptible to measles is high. Hence, we assume that $S(0) = 20,000,000$, one-third of the South African population. We further assume that $M(0) = 250,000$ and $R(0) = 500$, thereby completing Table 2 of the initial conditions. The values of the parameters are assumed, estimated or quoted in Table 1 which implies that $\mathcal{R}_0 = 1.0226$. In particular, since the annual natural mortality per 1000 inhabitants in South Africa for 2021 was 11.43, and assuming that the carrying capacity, Λ/d, for the MSEIR model is $60,000,000$, the total population of South Africa, we estimate the recruitment constant, Λ, to 1,879.

The numerical result provided on Fig. 1 highlights the usefulness of the vaccination to mitigate the number of infected individuals and to increase the total population, though $\mathcal{R}_0 = 1.0226$. It is seen that the vaccination profile should be at its highest value during 43 days before dropping down to 0 at the final time. This is consistent with Eq. (10) in the specific form (32) and (35).

For comparison purpose, we show on Fig. 2 the solution of the optimal control problem defined in (26) using the classical forward–backward-sweep Euler scheme. We choose the step size $\Delta t = 0.08$ for both the state variable and the adjoint equations. The inefficiency of this numerical method is apparent. More precisely, both curves of latent and infected individuals lead to negative solutions. Moreover, the vaccination profile reduces to zero, thereby suggesting that no control was implemented, which is unrealistic. This observation is a new fact in the literature in supporting the superiority of the NSFD-FBSM over the classical Euler-based FBSM.

5. Ebola patch model with optimal exit screening and vaccination

5.1. Ebola patch model with exit screening

In the paper [33], the authors investigated the transmission dynamics and optimal control of the Ebola Virus Disease (EVD) in a complex but realistic setting of patch model in the light of the 2014–2016 West Africa EVD that arose simultaneously in three

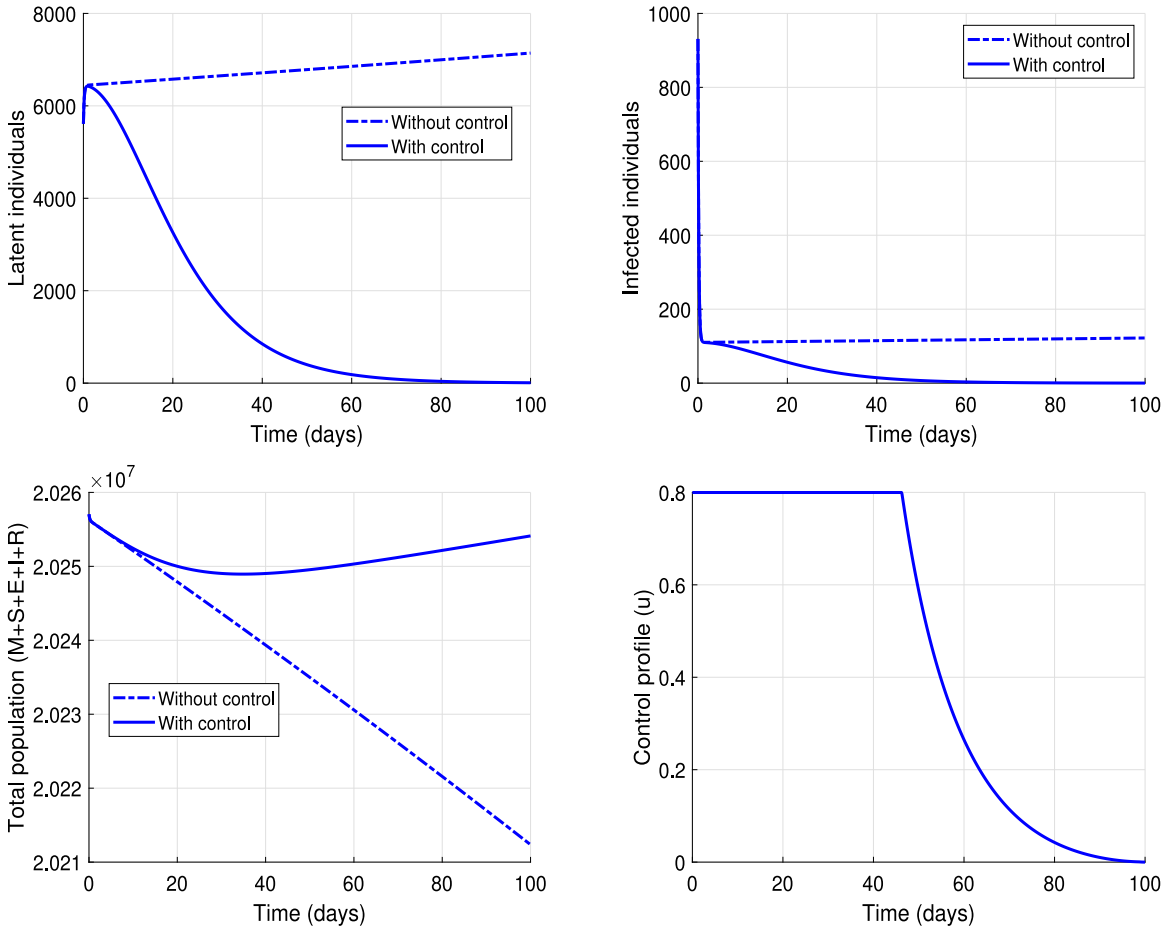


Fig. 1. Optimal vaccination solved by the NSFD-FBSM with $\Delta t = 2$ for the state variables and $\Delta t = 0.005$ for the adjoint variables ($\mathcal{R}_0 = 1.0226$). This figure is plotted with $A = 3, q = 500$ (the other values of the parameters are in Table 1).

countries (viz. Guinea, Liberia and Sierra Leone) to and from which migrations and travels by road, sea and air were considerable. Their models took into account the entry-exit screening and the quarantine measures. In this paper, we restrict ourselves to the exit screening only as recommended by WHO. The model involves the variables S_i, E_i, I_i, Q_i, P_i and R_i (for each patch i), the definitions of which are given on Table 3. The flow diagram for the model is depicted on Fig. 3.

$$
\begin{cases}
\dfrac{dS_i(t)}{dt} &= \Lambda_i - \dfrac{\beta_i(I_i + \nu_i D_i)S_i}{N_i} - \mu_i S_i - \displaystyle\sum_{j\neq i}^{n} a_{ji} S_i + \sum_{j\neq i}^{n} a_{ij}(1-\eta_j^S)S_j \\
&\quad + \displaystyle\sum_{j=1}^{n}(1-\widetilde{\phi}_j(E_j))\upsilon_j \xi_{ij} Q_j, \\
\dfrac{dE_i(t)}{dt} &= \dfrac{\beta_i(I_i + \nu_i D_i)S_i}{N_i} - \mu_i E_i - \alpha_i E_i - \displaystyle\sum_{j\neq i}^{n} a_{ji} E_i + \sum_{j\neq i}^{n} a_{ij}(1-\eta_j^E)E_j, \\
\dfrac{dI_i(t)}{dt} &= \alpha_i E_i - (\mu_i + \delta_i + \gamma_i)I_i, \\
\dfrac{dD_i(t)}{dt} &= (\mu_i + \delta_i)I_i - b_i D_i, \\
\dfrac{dQ_i(t)}{dt} &= \displaystyle\sum_{j\neq i}^{n} a_{ji}\eta_i^E E_i + \sum_{j\neq i}^{n} a_{ji}\eta_i^S S_i - (\mu_i + \upsilon_i)Q_i, \\
\dfrac{dP_i(t)}{dt} &= \widetilde{\phi}_i(E_i)\upsilon_i Q_i - (\mu_i + \psi_i + \theta_i)P_i, \\
\dfrac{dR_i(t)}{dt} &= \gamma_i I_i + \theta_i P_i - \mu_i R_i,
\end{cases}
\tag{38}
$$

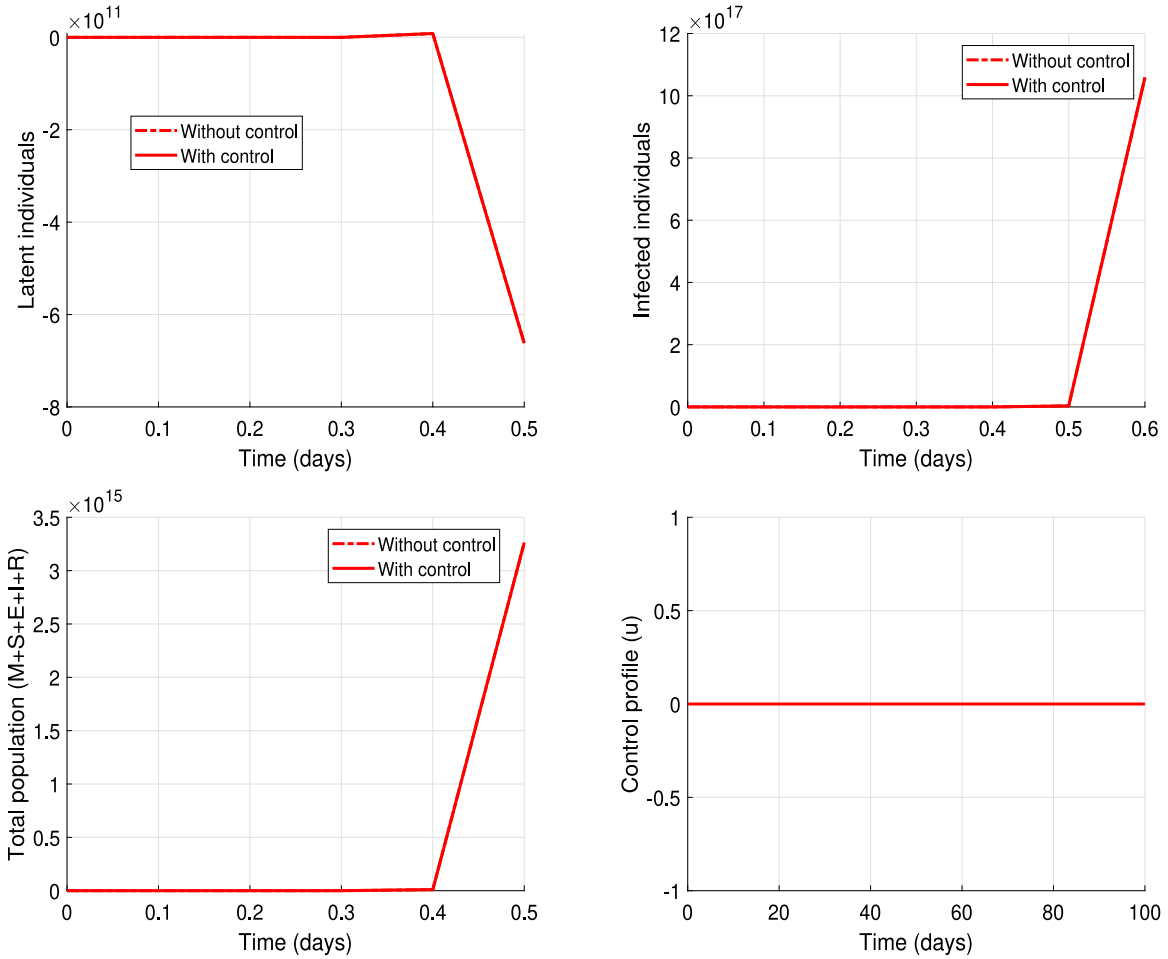


Fig. 2. Optimal vaccination solved with the classical Euler-based FBSM with $\Delta t = 0.08$ for the state and adjoint variables. This figure is plotted with $A = 3$ (the other values of the parameters are in Table 1). The dynamical inconsistency of the classical scheme with respect to the positivity of solutions and the impact of the vaccination intervention is apparent.

where

$$\widetilde{\phi}_i(e) = \begin{cases} 0 \text{ if } e \leq 0, \\ \phi_i \text{ (where } \phi_i \leq 1 \text{ is a positive constant) if } e > 0, \end{cases} \tag{39}$$

the constant ϕ_i being the probability for a quarantined individual to be infected. The other definitions of the model parameters are provided in Table 4. For convenience, we introduce the following notation:

$$\begin{aligned}
&\mathcal{E} = (S, E, I, D, Q, P, R) \in \mathbb{R}_+^{7n} \text{ where } S = (S_1, \dots, S_n), E = (E_1, \dots, E_n), I = (I_1, \dots, I_n), \\
&D = (D_1, \dots, D_n), Q = (Q_1, \dots, Q_n), P = (P_1, \dots, P_n), R = (R_1, \dots, R_n), \\
&H_i = S_i + E_i + I_i + Q_i + P_i + R_i, \;\; N_i = H_i + D_i, \; \mathbf{H} = \sum_{i=1}^{n} H_i; \\
&\mathbf{D} = \sum_{i=1}^{n} D_i; \; \Lambda = \sum_{i=1}^{n} \Lambda_i, \; \Upsilon = \sum_{i=1}^{n} (\mu_i + \delta_i), \; \mu_m = \min_{1 \leq i \leq n} \{\mu_i\}, \; k_i = (\mu_i + \delta_i + \gamma_i), \\
&b_m = \min_{1 \leq i \leq n} \{b_i\}, \; \mu_M = \max_{1 \leq i \leq n} \{\mu_i + \delta_i + \psi_i\}, \; \omega_i = \mu_i b_i k_i + \mu_i b_i \alpha_i + \mu_i \alpha_i (\mu_i + \delta_i) + \gamma_i b_i \alpha_i, \\
&a^M = \max_{1 \leq i \leq n} \left(\beta_i (1 + \nu_i) + \mu_i + \sum_{j=1}^{n} a_{ji} \right); \; \alpha^M = \max_{1 \leq i \leq n} \left(\mu_i + \alpha_i \right); \; \gamma^M = \max_{1 \leq i \leq n} \left(\mu_i + \delta_i + \gamma_i \right); \\
&b^M = \max_{1 \leq i \leq n} \left(b_i \right); \; \upsilon^M = \max_{1 \leq i \leq n} \left(\mu_i + \upsilon_i \right); \; \theta^M = \max_{1 \leq i \leq n} \left(\mu_i + \psi_i + \theta_i \right); \; \mu^M = \max_{1 \leq i \leq n} \left(\mu_i \right).
\end{aligned} \tag{40}$$

Table 3
Variables of the model for each patch i.

Classes	Description
S_i	Susceptible individuals who did not undergo screening or who were negatively screened.
E_i	Latent individuals coming from the infection of the individuals in S_i.
I_i	EVD symptomatic cases who left the latent compartment E_i.
D_i	Ebola-death cases.
Q_i	Travellers positively screened at the exit borders and quarantined.
P_i	Isolated individuals who failed to travel due to a positive screening, followed by a positive diagnosis at the exit borders.
R_i	Individuals who recover from EVD.

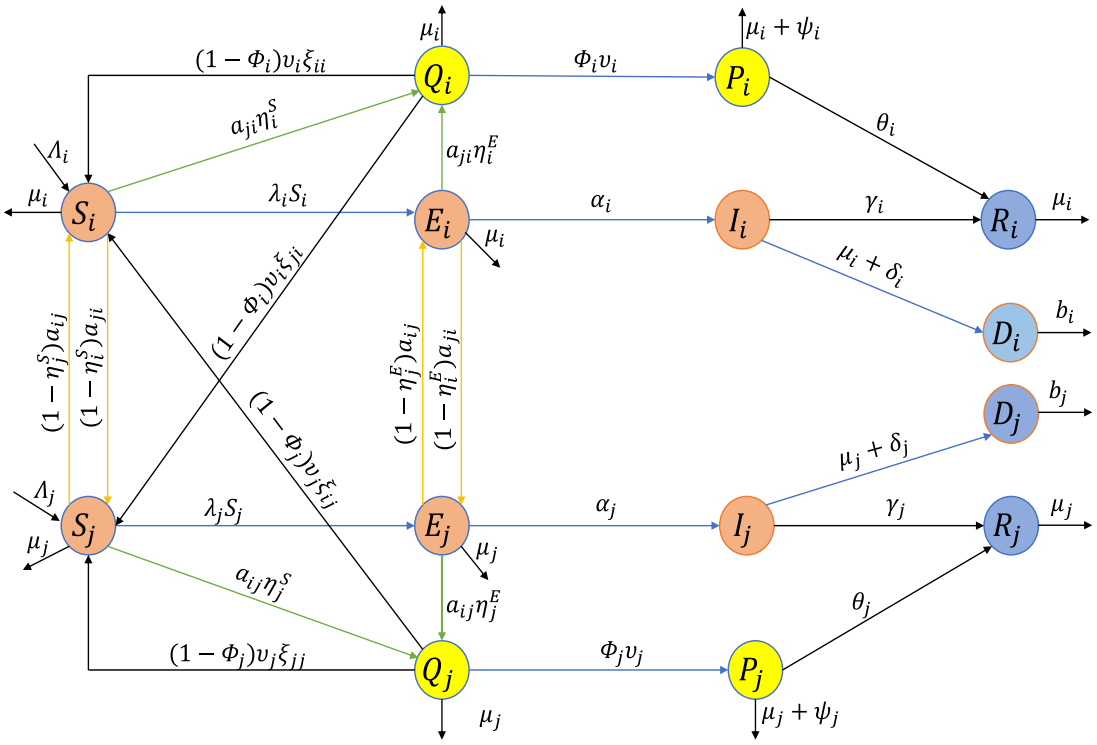


Fig. 3. Flow diagram between compartments of two patches i and j ($i \neq j$) for Model (38).

With the step function $\widetilde{\phi}_i$ in (39), it can be shown by some algebraic computation that System (38) has a unique disease-free equilibrium, DFE$\equiv \mathcal{E}_0$, given in terms of the notation (40) by

$$\mathcal{E}_0 = (S^0, 0, 0, 0, Q^0, 0, 0) \in \mathbb{R}_+^{7n}. \tag{41}$$

In [33], the authors computed the control reproduction number, $\mathcal{R}_c$, of Model (38) using the next generation matrix. They also considered the more explicit threshold

$$\mathcal{T} = \max_{1\leq i\leq n} \frac{\beta_i \alpha_i (b_i + \nu_i(\mu_i + \delta_i))}{b_i k_i \left((\mu_i + \alpha_i) + \sum_{j\neq i}^{n} a_{ji}\eta_i^E \right)}, \tag{42}$$

which reduces to the basic reproduction number of Model (38) in the particular case when all susceptible travellers are negatively screened, while all latent individuals are quarantined i.e $Q_i^0 = 0$. Here is the result established in [33] for the qualitative properties of Model (38).

Theorem 9.

1. *Model (38) is a dynamical system on the biologically feasible region*

$$\Gamma = \left\{ \mathcal{E} = (S, E, I, D, Q, P, R) \in \mathbb{R}_+^{7n} : \mathbf{H} \leq \frac{\Lambda}{\mu_m} \text{ and } \mathbf{D} \leq \frac{\Upsilon \Lambda}{\mu_m b_m} \right\},$$

Table 4
Parameters of the model.

Parameters	Epidemiological interpretation	Units
a_{ij}	Rate of susceptible/latent individuals of patch j who wish to migrate to patch i.	week^{-1}
μ_i	Natural mortality rate in patch i.	week^{-1}
Λ_i	Constant recruitment of susceptible in patch i.	indiv.week^{-1}
β_i	Effective transmission rate of EVD in patch i due to individuals in I_i compartment.	indiv.week^{-1}
b_i	Burial rate of Ebola-deceased in patch i.	week^{-1}
γ_i	Recovery rate of infected who belong to the I_i compartment.	week^{-1}
θ_i	Recovery rate of individuals who belong to the P_i compartment.	week^{-1}
α_i	Exit rate of the E_i compartment to the I_i compartment.	week^{-1}
ν_i	Modification parameter for the infectiousness of the Ebola-deceased.	–
η_i^S	Proportion of susceptible individuals in S_i who are positively screened at the exit-border of patch i.	–
η_i^E	Proportion of latent individuals in E_i who are positively screened at the exit of patch i.	–
δ_i	Mortality rate due to EVD of infected individuals in patch i who belong to the I_i compartment.	–
ψ_i	Mortality rate due to EVD of infected in patch i who belong to the P_i compartment.	week^{-1}
υ_i	Exit rate from the Q_i compartment by any means different from the death.	week^{-1}
$\widetilde{\phi}_i(E_i)\upsilon_i Q_i$	Proportion of quarantined individuals who are positively diagnosed.	indiv.week^{-1}
ξ_{ij}	Rate at which the quarantined who are negatively diagnosed in patch j left patch j to patch i ($j \neq i$).	week^{-1}
ξ_{ii}	Rate at which the quarantined who are negatively diagnosed in patch i cancel their trip.	week^{-1}

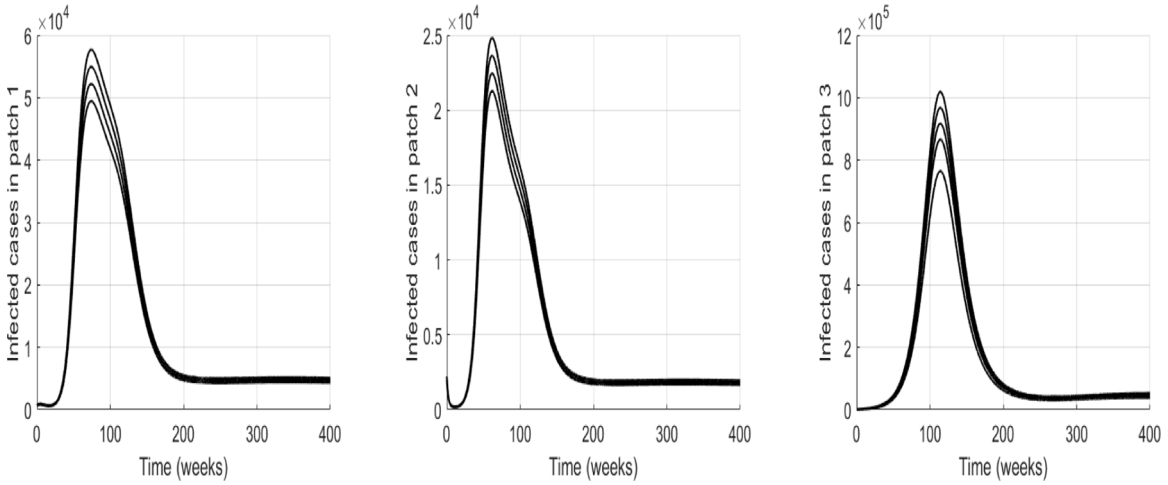


Fig. 4. Numerical simulations suggesting, for $\mathcal{R}_c > 1$, the existence of a positive interior equilibrium and its stability. The values to plot these figures are in Table 5. With these values, $\mathcal{R}_c = 3.9537 > 1$, $\mathcal{T} = 4.2333 > 1$.

which is attractive.

2. *The DFE, $\mathcal{E}_0$, is unstable whenever $\mathcal{R}_c > 1$. It is locally asymptotically stable if $\mathcal{R}_c < 1$. In the latter case, $\mathcal{E}_0$ is globally asymptotically stable (GAS) provided that the exit screening is 100% negative i.e $\eta_i^S = \eta_i^E = 0$ for all patches i.*
3. *The DFE is GAS if $\mathcal{T} < 1$.*

Remark 10. The existence and stability of endemic and or boundary equilibria in the case when $\mathcal{R}_c > 1$, and particularly when $\mathcal{R}_c < 1 < \mathcal{T}$, are investigated numerically as seen on Figs. 4 and 5, respectively.

The exit screening which is the main intervention that WHO recommended for the 2014–2016 Ebola outbreak in Guinea, Liberia and Sierra Leone can be detrimental to the country that implements it as far as the number of infected individuals is concerned. To address this concern, we combine the exit screening with the vaccination as a supplement intervention. Such a strategy is sound

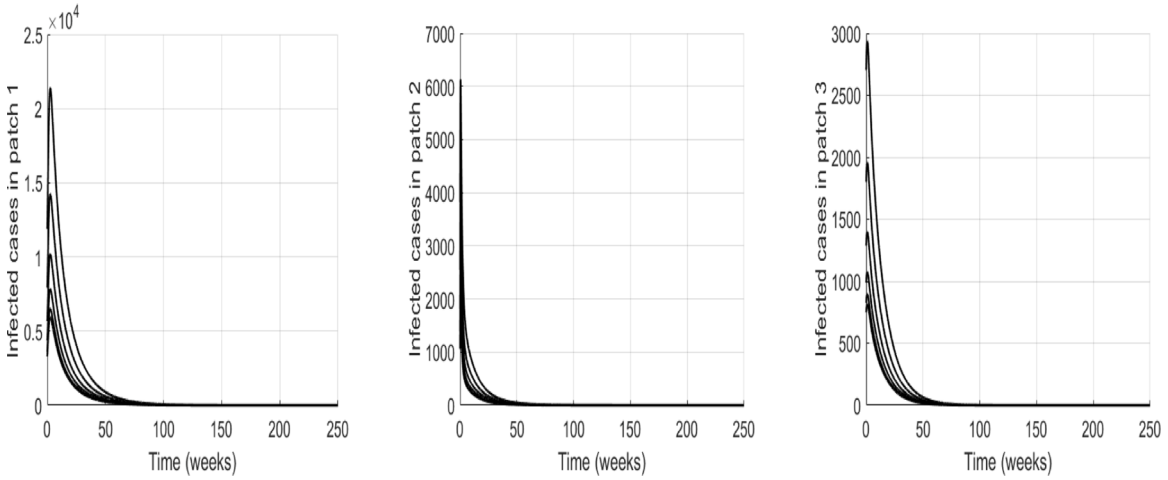


Fig. 5. Numerical simulations suggesting the GAS of the DFE when $\mathcal{R}_c < 1 < \mathcal{T}$. Here $\beta_2 = 0.21329; \mathcal{R}_c = 0.9312 < 1, \mathcal{T} = 1.1287 > 1$. The other values for the simulations are as in Table 5.

as the Ebola vaccination is increasingly used since the discovery of the rVsV-ZEBOV-GP Ebola vaccine and the Ad26.ZEBOV/MVA-BN-Filo vaccine which occupied a prominent place in the control of the 2018–2020 EVD outbreak in the Democratic Republic of Congo [34,35].

We assume that the exit screening implemented in Patch i targets only the latent travellers at the time-dependent rate $\eta_i(t)$, and we denote by $\sigma_i(t)$ the time-dependent rate for the vaccination in Patch i. As the EVD vaccine is not 100% perfect, among the $\sigma_i(t)S_i$ individuals vaccinated, we assume that, only a fraction κ acquired immunity. With this in mind, Model (38) becomes for $i = 1, \dots, n$:

$$\begin{cases} \dot{S}_i(t) &= \Lambda_i - \dfrac{\beta_i(I_i + \nu_i D_i)S_i}{N_i} - \mu_i S_i + \displaystyle\sum_{j\neq i}^{n} a_{ij}S_j - \sum_{j\neq i}^{n} a_{ji}S_i - \kappa\sigma_i(t)S_i, \\ \dot{E}_i(t) &= \dfrac{\beta_i(I_i + \nu_i D_i)S_i}{N_i} - \mu_i E_i - \alpha_i E_i + \displaystyle\sum_{j\neq i}^{n} a_{ij}(1-\eta_j(t))E_j - \sum_{j\neq i}^{n} a_{ji}E_i, \\ \dot{I}_i(t) &= \alpha_i E_i - (\mu_i + \delta_i + \gamma_i)I_i, \\ \dot{D}_i(t) &= (\mu_i + \delta_i)I_i - b_i D_i, \\ \dot{Q}_i(t) &= \displaystyle\sum_{j\neq i}^{n} a_{ji}\eta_i(t)E_i - (\mu_i + \upsilon_i)Q_i, \\ \dot{P}_i(t) &= \upsilon_i Q_i - (\mu_i + \psi_i + \theta_i)P_i, \\ \dot{R}_i(t) &= \kappa\sigma_i(t)S_i + \gamma_i I_i + \theta_i P_i - \mu_i R_i \\ S_i(0) &= S_i^0 \geq 0, \;\; E_i(0) = E_i^0 \geq 0, \;\; I_i(0) = I_i^0 \geq 0, \;\; D_i(0) = D_i^0 \geq 0, \\ Q_i(0) &= Q_i^0 \geq 0, \;\; P_i(0) = P_i^0 \geq 0, \;\; R_i(0) = R_i^0 \geq 0. \end{cases} \tag{43}$$

Our aim is to minimize both the cost of the control measures and the number of infected individuals. Therefore, we can define the objective functional by

$$J \equiv J(x, \sigma, \eta) = \int_0^T f(t, x, \eta, \sigma), \;\; \text{with } f(t, x, \eta, \sigma) := [\sum_{i=1}^{n} w_i E_i(t) + \frac{d_i}{2}{\sigma_i}^2(t) + \frac{c_i}{2}\eta_i^2(t)]dt, \tag{44}$$

where T is the maximum duration of the implementation of these two measures, w_i is the weight factor associated with latent humans E_i; d_i and c_i are the weight factors linked to the control variables σ_i and η_i, respectively. The control set is

$$U = \{[(\sigma_i)_{i=1}^{i=n}, (\eta_i)_{i=1}^{i=n}], \; \forall i : \; \sigma_i, \eta_i \;\; \text{Lebesgue measurable}, \; 0 \leq \sigma_i(t), \eta_i(t) \leq 1, \;\; \text{a.e. on } [0, T]\}. \tag{45}$$

The Hamiltonian of the optimal control problem of minimizing $J(x,\sigma,\eta)$ in (44) subject to (43) is

$$\begin{aligned}\mathcal{H} = & \sum_{i=1}^{n} w_i E_i(t) + \frac{d_i}{2}{\sigma_i}^2(t) + \frac{c_i}{2}\eta_i^2(t) + z_{1i}[\Lambda_i - \frac{\beta_i(I_i+\nu_i D_i)S_i}{N_i} - \mu_i S_i + \sum_{j=1}^{n} a_{ij}S_j \\ & - \sum_{j=1}^{n} a_{ji}S_i - \sigma_i(t)S_i] + z_{2i}[\frac{\beta_i(I_i+\nu_i D_i)S_i}{N_i} - \mu_i E_i - \alpha_i E_i + \sum_{j=1}^{n} a_{ij}(1-\eta_j(t))E_j \\ & - \sum_{j=1}^{n} a_{ji}E_i] + z_{3i}[\alpha_i E_i - (\mu_i+\delta_i+\gamma_i)I_i] + z_{4i}[(\mu_i+\delta_i)I_i - b_i D_i] \\ & + z_{5i}[\sum_{j=1}^{n} a_{ji}\eta_i(t)E_i - (\mu_i+\upsilon_i)Q_i] + z_{6i}[\upsilon_i Q_i - (\mu_i+\psi_i+\theta_i)P_i] \\ & + z_{7i}[\sigma_i(t)\kappa S_i(t) + \gamma_i I_i + \theta_i P_i - \mu_i R_i],\end{aligned} \tag{46}$$

where the right-hand side of (43), denoted by $g(t,x,\eta,\sigma)$, and the integrand, $f(t,x,\eta,\sigma)$, are written explicitly. It can be shown that the functions f and g satisfy all the assumptions used in Theorems 1 and 2. In particular, the choice of the quadratic terms σ_i^2 and η_i^2 guarantees that the objective functional J is convex, while the behaviour of g stated in Theorem 2 can be obtained as we did for the $MSEIR$ optimal control model. Therefore, we have the existence and characterization result below.

Theorem 11.

1. *Let (η^*,σ^*) be an optimal control of (43) with an associated state $x^*_{\eta,\sigma}$. Then, there exists a differentiable adjoint function $z(t) : [0,T] \to \mathbb{R}^{7n}$, solution of the adjoint system*

$$\begin{cases} \dot{z}_{1i}(t) = & -\frac{\partial\mathcal{H}}{\partial S_i} = \beta_i\frac{(I_i+\nu_i D_i)}{N_i}(z_{1i}-z_{2i}) + \mu_i z_{1i} + z_{1i}\sum_{j=1}^{n} a_{ji} + \kappa\sigma_i(t)z_{1i} \\ & -z_{7i}\sigma_i(t)\kappa - \sum_{j=1,j\neq i}^{n} z_{1j}a_{ji}, \\ \dot{z}_{2i}(t) = & -\frac{\partial\mathcal{H}}{\partial E_i} = -w_i + z_{2i}[\mu_i+\alpha_i+\sum_{j=1}^{n} a_{ji}] - z_{3i}\alpha_i - z_{5i}\sum_{j=1}^{n} a_{ji}\eta_i(t) \\ & - \sum_{j=1,j\neq i}^{n} z_{2j}a_{ji}(1-\eta_i(t)), \\ \dot{z}_{3i}(t) = & -\frac{\partial\mathcal{H}}{\partial I_i} = \frac{\beta_i S_i}{N_i}(z_{1i}-z_{2i}) + z_{3i}(\mu_i+\delta_i+\gamma_i) - z_{4i}(\mu_i+\delta_i) - z_{7i}\gamma_i, \\ \dot{z}_{4i}(t) = & -\frac{\partial\mathcal{H}}{\partial D_i} = \frac{\beta_i\nu_i S_i}{N_i}(z_{1i}-z_{2i}) + z_{4i}b_i, \\ \dot{z}_{5i}(t) = & -\frac{\partial\mathcal{H}}{\partial Q_i} = z_{5i}(\mu_i+\upsilon_i) - z_{6i}\upsilon_i, \\ \dot{z}_{6i}(t) = & -\frac{\partial\mathcal{H}}{\partial P_i} = z_{6i}(\mu_i+\psi_i+\theta_i) - z_{7i}\theta_i, \\ \dot{z}_{7i}(t) = & -\frac{\partial\mathcal{H}}{\partial R_i} = z_{7i}\mu_i, \\ z_{li}(T) = & \ 0,\ l=1,\dots,7,\ i=1,\dots,n. \end{cases} \tag{47}$$

   such that $\mathcal{H}(t,x,\eta,\sigma) \geq \mathcal{H}(t,x^*_{\eta^*,\sigma^*},\eta^*,\sigma^*)$.
2. *There exists a unique control $(\sigma^*,\eta^*) \in U$ such that the cost functional defined by (44) is minimized.*
3. *These controls can be expressed, $\forall\, i=1,\dots,n$, as*

$$\eta_i^*(t) = \begin{cases} 1 & \text{if} \quad 0 \leq t < T^*_{\eta_i}, \\ \frac{\sum_{j=1,j\neq i}^{n} a_{ji}(z_{2j}-z_{5i})E_i}{c_i}, & \text{if} \quad T^*_{\eta_i} \leq t \leq T^{**}_{\eta_i}, \\ 0 & \text{if} \quad T^{**}_{\eta_i} < t \leq T. \end{cases} \tag{48}$$

   and

$$\sigma_i^*(t) = \begin{cases} 1 & \text{if} \quad 0 \leq t < T^*_{\sigma_i}, \\ \frac{S_i\kappa(z_{1i}-z_{7i})}{d_i}, & \text{if} \quad T^*_{\sigma_i} \leq t \leq T^{**}_{\sigma_i}, \\ 0 & \text{if} \quad T^{**}_{\sigma_i} < t \leq T. \end{cases} \tag{49}$$

   where, like in the case of the MSEIR optimal control problem, $T^*_{\eta_i}$ & $T^*_{\sigma_i}$ and $T^{**}_{\eta_i}$ & $T^{**}_{\sigma_i}$ are defined as T^* and T^{**}, respectively.

Going forward, we want to solve numerically the optimal control problem of minimizing J in (44) subject to (43) in its equivalent form (43), (47), (48) and (49). The starting point is to consider the continuous FBSM, (18), which here reads as follows: For the iterations $m \geq 0$, we choose an initial guess $\eta^0 = \eta^0(t)$ and $\sigma^0 = \sigma^0(t)$ and seek for $x^{(m+1)}, z^{(m+1)}, \eta^{(m+1)}$ and $\sigma^{(m+1)}$ solutions to the

system:

$$\begin{cases} \dfrac{x^{(m+1)}(t)}{dt} = g(t, x^{(m+1)}(t), \eta^{(m)}(t), \sigma^{(m)}(t)), & x^{(m+1)} = x(0) \\ \dfrac{dz^{(m+1)}(t)}{dt} = \Psi(t, x^{m+1}(t), \eta^{(m)}(t), \sigma^{(m)}(t)), & z^{(m+1)}(T) = 0 \\ \eta^{(m+1)}(t) := \varphi_1(t, x^{(m+1)}(t), z^{(m+1)}(t)), \\ \sigma^{(m+1)}(t) := \varphi_2(t, x^{(m+1)}(t), z^{(m+1)}(t)), \end{cases} \tag{50}$$

where φ_1, φ_2 are functions that come from (48) & (49), and

$$\begin{aligned} \Psi(t, x^{(m+1)}(t), \eta^{(m)}(t), \sigma^{(m)}(t)) = \quad & -(f_x(t, x^{(m+1)}(t), \eta^{(m)}(t), \sigma^{(m)}(t)) \\ & + z^{(m+1)} g_x(t, x^{(m+1)}(t), \eta^{(m)}(t), \sigma^{(m)}(t))). \end{aligned}$$

With the discretizations t_k of $[0, T]$, we propose the following Euler-based NSFD-FBSM.

- For $m = 0$, we choose the initial guess $\eta^{k,0}, \sigma^{k,0},\ k = 0, 1, \dots, p$.
- For $m \geq 0$:
  - We compute $x^{k+1,(m+1)}$ by the Nonstandard Forward Euler scheme for (43),

$$\frac{x^{k+1,(m+1)} - x^{k,(m)}}{r} = g(t_k, x^{k,(m+1)}, \tau^{k,(m)}), \quad x_0^{k,(m+1)}(0) = x_0^k,\ k = 0, 1, \dots, p-1,$$

    which, $\forall\ i = 1, \dots, n$, corresponds to

$$\begin{cases} \dfrac{S_i^{k+1,(m+1)} - S_i^{k,(m)}}{r} = \Lambda_i - \lambda_i^{k,(m+1)} S_i^{k,(m+1)} - \mu_i S_i^{k,(m+1)} - \displaystyle\sum_{j=1}^{n} a_{ji} S_i^{k,(m+1)} \\ \qquad + \displaystyle\sum_{j=1}^{n} a_{ij} S_j^{k,(m+1)} - \kappa \sigma_i^{k,(m)} S_i^{k,(m+1)}, \\ \dfrac{E_i^{k+1,(m+1)} - E_i^{k,(m)}}{r} = \lambda_i^{k,(m+1)} S_i^{k,(m+1)} - \mu_i E_i^{k,(m+1)} - \alpha_i E_i^{k,(m+1)} - \displaystyle\sum_{j=1}^{n} a_{ji} E_i^{k,(m+1)} \\ \qquad + \displaystyle\sum_{j=1}^{n} a_{ij} (1 - \eta_j^{k,(m)}) E_j^{k,(m+1)}, \\ \dfrac{I_i^{k+1,(m+1)} - I_i^{k,(m)}}{r} = \alpha_i E_i^{k,(m+1)} - (\mu_i + \delta_i + \gamma_i) I_i^{k,(m+1)}, \\ \dfrac{D_i^{k+1,(m+1)} - D_i^{k,(m)}}{r} = (\mu_i + \delta_i) I_i^{k,(m+1)} - b_i D_i^{k,(m+1)}, \\ \dfrac{Q_i^{k+1,(m+1)} - Q_i^{k,(m)}}{r} = \displaystyle\sum_{j=1}^{n} a_{ji} \eta_i^{k,(m)} E_i^{k,(m+1)} - \mu_i Q_i^{k,(m+1)} - \upsilon_i Q_i^{k,(m+1)}, \\ \dfrac{P_i^{k+1,(m+1)} - P_i^{k,(m)}}{r} = \upsilon_i Q_i^{k,(m+1)} - (\mu_i + \psi_i + \theta_i) P_i^{k,(m+1)}, \\ \dfrac{R_i^{k+1,(m+1)} - R_i^{k,(m)}}{r} = \kappa \sigma_i^{k,(m)} S_i^{k,(m+1)} + \gamma_i I_i^{k,(m+1)} + \theta_i P_i^{k,(m+1)} - \mu_i R_i^{k,(m+1)}, \end{cases} \tag{51}$$

    where r is defined by (14) with

$$q \geq \min\left(\frac{1}{a^M}, \frac{1}{\alpha^M}, \frac{1}{\gamma^M}, \frac{1}{b^M}, \frac{1}{\upsilon^M}, \frac{1}{\theta^M}, \frac{1}{\mu^M}\right) \tag{52}$$

    and satisfying the analog of (20) for the model (43).
  - The adjoint discrete system is defined through the classical backward Euler scheme as follows: for $k = p-1, \dots, 0$

$$\frac{z^{k+1,(m+1)} - z^{k,(m+1)}}{\Delta t} = \Psi(t_{k+1}, x^{k+1,(m+1)}, z^{k+1,(m+1)}, \eta^{k+1,(m)}, \sigma^{k+1,(m)}),\ z^{p,(m+1)}(T) = 0,$$

This gives the following discrete system for $l = 1, 2, \dots, 7, i = 1, 2, \dots, n$ and $k = p-1, p-2, \dots, 0$:

$$
\begin{cases}
\dfrac{z_{1i}^{k+1,(m+1)} - z_{1i}^{k,(m+1)}}{\Delta t} = & \dfrac{\beta_i (I_i^{k+1,(m+1)} + \nu_i D_i^{k+1,(m+1)}) S_i^{k+1,(m+1)}}{N_i^{k+1,(m+1)}} (z_{1i}^{k+1,(m+1)} - z_{2i}^{k+1,(m+1)}) \\
& + \mu_i z_{1i}^{k+1,(m+1)} + z_{1i}^{k+1,(m+1)} \sum_{j=1}^{n} a_{ji} + \kappa \sigma_i^{k+1,(m)} z_{1i}^{k+1,(m+1)} \\
& - z_{7i}^{k+1,(m+1)} \sigma_i^{k+1,(m)} \kappa - \sum_{j=1, j\neq i}^{n} z_{1j}^{k+1,(m+1)} a_{ji}, \\
\dfrac{z_{2i}^{k+1,(m+1)} - z_{2i}^{k,(m+1)}}{\Delta t} = & -w_i + z_{2i}^{k+1,(m+1)} \left[\mu_i + \alpha_i + \sum_{j=1}^{n} a_{ji} \right] - z_{3i}^{k+1,(m+1)} \alpha_i \\
& - z_{5i}^{k+1,(m+1)} \sum_{j=1}^{n} a_{ji} \eta_i^{k+1,(m)} - \sum_{j=1, j\neq i}^{n} z_{2j}^{k+1,(m+1)} a_{ji} (1 - \eta_i^{k+1,(m)}), \\
\dfrac{z_{3i}^{k+1,(m+1)} - z_{3i}^{k,(m+1)}}{\Delta t} = & \dfrac{\beta_i S_i^{k+1,(m+1)}}{N_i^{k+1,(m+1)}} (z_{1i}^{k+1,(m+1)} - z_{2i}^{k+1,(m+1)}) + z_{3i}^{k+1,(m+1)} (\mu_i + \delta_i + \gamma_i) \\
& - z_{4i}^{k+1,(m+1)} (\mu_i + \delta_i) - z_{7i}^{k+1,(m+1)} \gamma_i, \\
\dfrac{z_{4i}^{k+1,(m+1)} - z_{4i}^{k,(m+1)}}{\Delta t} = & \dfrac{\beta_i \nu_i S_i^{k+1,(m+1)}}{N_i^{k+1,(m+1)}} (z_{1i}^{k+1,(m+1)} - z_{2i}^{k+1,(m+1)}) + z_{4i}^{k+1,(m+1)} b_i, \\
\dfrac{z_{5i}^{k+1,(m+1)} - z_{5i}^{k,(m+1)}}{\Delta t} = & z_{5i}^{k+1,(m+1)} (\mu_i + \upsilon_i) - z_{6i}^{k+1,(m+1)} \upsilon_i, \\
\dfrac{z_{6i}^{k+1,(m+1)} - z_{6i}^{k,(m+1)}}{\Delta t} = & z_{6i}^{k+1,(m+1)} (\mu_i + \psi_i + \theta_i) - z_{7i}^{k+1,(m+1)} \theta_i, \\
\dfrac{z_{7i}^{k+1,(m+1)} - z_{7i}^{k,(m+1)}}{\Delta t} = & z_{7i}^{k+1,(m+1)} \mu_i.
\end{cases}
\tag{53}
$$

Note that except from $z_{2i}^{k,(m+1)}$, all the terms $z_{li}^{k,(m+1)}$ with $l \neq 2$ are equal to zero due to the transversality condition. The discrete analog of part of Theorem 9 is as follows:

Theorem 12. *Assume that $\eta(t)$ and $\sigma(t)$ are constant. Then, the NSFD scheme (51) is dynamically consistent with the continuous Model (38) in the sense that it is a discrete dynamical system on the biologically feasible region Γ. Moreover, under the conditions (20) and (52), the disease-free fixed (DFF) point of the NSFD scheme of (51) is elementary stable in the sense that the disease-free equilibrium of the continuous model coincides with the DFF and both of them are LAS if the control reproduction number is less than one.*

The first part of Theorem 12 is obtained by the construction of the NSFD scheme under consideration. The second part is essentially based on the Lyapunov indirect method, which amounts to showing that the spectral radius of the Jacobian matrix of the defining function of disease-free fixed point is less than 1 whenever the control reproduction number is less than 1. This is precisely the case under the conditions (20) and (52), in view of an intrinsic relation that holds between this Jacobian matrix and that of the continuous model (38) evaluated at the disease-free equilibrium [8].

5.2. Numerical simulations

The numerical simulations for our NSFD-FBSM (51), (52) and (53) for the optimal control problem that combines the vaccination and exit screening measures will be implemented in Guinea (patch 1), Liberia (patch 2) and Sierra Leone (patch 3), the countries that were more affected by the 2014–2016 EVD outbreak. The parameters to be used were mostly estimated in [33] from real data and they are gathered in Tables 5–6. We solve the optimality system during forty weeks. For comparison purpose, we also use the classical Euler-based FBSM.

Fig. 6 should be read in conjunction with Table 7 regarding the role of T^* and T^{**}, the times needed to include the bounds of the controls as explained in Eqs. (48) & (49). Though the exit screening is implemented in an optimal manner, the solutions curves on Fig. 6 suggest that the impact of the screening intervention alone is weak. This reinforces the need to combine it with another control strategy such as the vaccination. The control profiles show that the exit screening has to be at its highest value in Guinea, Liberia and Sierra Leone during 16 weeks, 38 weeks and 19 weeks, respectively, before dropping to their lowest bounds at the final time. The optimal vaccination must be implemented in Guinea, Liberia and Sierra Leone during 34 weeks, 39 weeks and 29 weeks, respectively, before decreasing until their lowest values at the end time. This figure highlights that the vaccination intervention is more efficient than the border measures, and justifies the implementation of the former for the control of EVD during the 2018–2020 DRC Kivu Outbreak [43].

On the other hand, we illustrate on Fig. 7 the same optimal control problem using the classical Euler-based FBSM with the same initial conditions and the step size $h = 0.05$. The superiority of the NSFD over the classical schemes has been abundantly studied in terms of the preservation of features of the continuous models such as boundedness of solutions, stability of equilibrium points and conservation laws [1,3,4,6,7,9,10]. In this work, the superiority of the NSFD-FBSM on the classical Euler scheme is observed on two additional accounts. Firstly, the latter produces negative latent individuals which is not acceptable. Secondly, all the curves merge and all the control profiles reduce to the constant function zero, which leads to an unrealistic situation that neither the exit screening nor the vaccination intervention has an impact on the control of the infection.

Table 5
Parameters values to simulate System (43). The parameters without source in the table were estimated in [33].

Par.	Values	Source	Val Fig. 4	Par.	Values	Source	Val Fig. 4
η_1^E	0.2967		0.5433	κ	0.5	[36]	
μ_1	0.0002		0.00004	υ_1	0.477		0.51868
β_1	0.1523		0.0015	β_2	0.01329		0.0006312
β_3	0.1615		0.3128	υ_2	2.6571		0.53906
ν_1	2.1556		0.508	ν_2	0.9219		3.0656
ν_3	1.1275		0.867	$\phi_i, \forall\, i$	0.022		0.022
δ_1	0.857	[35]	0.857	δ_2	0.75	[37]	0.075
δ_3	0.5	[38]	0.5	υ_3	0.6682		0.5764
ψ_1	0.3	[39]	0.3	ψ_2	0.4	[40]	0.04
ψ_3	0.5	[38]	0.5	ξ_{21}	0.0145		0.0764
ξ_{31}	0.4516		0.4676	ξ_{12}	0.8712		0.5018
ξ_{11}	0.03		0.4557	ξ_{22}	0.0339		0.5109
ξ_{33}	0.0959		0.7053	$d_i, \forall\, i$	200		
ξ_{32}	0.4072		0.4873	ξ_{13}	0.2677		0.2328
ξ_{23}	0.9466		0.0612	a_{21}	0.000064×50		0.000284
a_{31}	0.0001×50		0.0121	a_{12}	0.00054×50		0.05548
a_{32}	0.0001×50		0.0150	a_{13}	0.00063×50		0.000122
a_{23}	0.000036×50		0.0131	b_3	0.5	[37,38]	0.5
b_1	1/2.01	[37,38]	1/2.01	b_2	1/4.5	[37]	1/4.5
γ_1	0.0059	[41]	0.059	γ_2	0.026767	[41]	0.6026767
θ_1	0.001120	[41]	0.75	θ_2	0.031486	[41]	0.075
θ_3	0.015743	[41]	0.75	γ_3	0.010038	[41]	0.010038
w_1	1			μ_2	0.0002		14/1000
μ_3	0.0002		10.17/1000	$\pi_i, \forall\, i$	0.03703	[42]	0.03703
α_1	1.2746		10.5239	α_2	4.6956		0.083333
α_3	0.5817		0.1	η_1^S	0.1065		0.21
η_2^S	0.2541		0.21	η_3^S	0.5383		0.2317
η_2^E	0.2366		0.226	η_3^E	0.1390		0.4229
w_1	0.002			c_1	0.125		
w_3	0.65			w_2	0.2		
c_2	0.5			c_3	0.68		

Table 6
Initial values of the variables for Model (38).

Countries	E(0)	I(0)	D(0)	Q(0)	P(0)	R(0)	Total
Guinea	330	286	286	286	286	286	1,760
Liberia	1,319	1,060	1,060	1,060	1,060	1,060	6,619
Sierra Leone	1,262	720	720	720	720	720	4,862

Table 7
Values of times $T_{c_i}^*$ and $T_{c_i}^{**}$ for the incorporation of bounds per type of control, $c_i = \eta_i$ (exit screening) or $c_i = \sigma_i$ (vaccination).

Exit screening	Guinea	Liberia	Sierra Leone
$T_{\eta_i}^*$	16	38	19
$T_{\eta_i}^{**}$	40	40	40
Vaccination	**Guinea**	**Liberia**	**Sierra Leone**
$T_{\sigma_i}^*$	34	39	29
$T_{\sigma_i}^{**}$	40	40	40

6. Conclusion and discussion

The nonstandard finite difference (NSFD) method was introduced by R. Mickens [3] more than three decades ago. The method has shown great potential and is becoming an established field to produce property preserving numerical schemes for various differential equation models of real life problems [3,6,7,10].

The motivation of this paper is twofold:

- To the authors best knowledge, the NSFD approach has not been used yet for optimal control problems.
- The lack of a suitable optimal control model for the 2014–2016 West Africa Ebola Virus Disease (EVD) outbreak that came with the unprecedented challenge of considerable migrations and travels of people inbound and outbound Guinea, Liberia and Sierra Leone, the three countries where the disease simultaneously erupted.

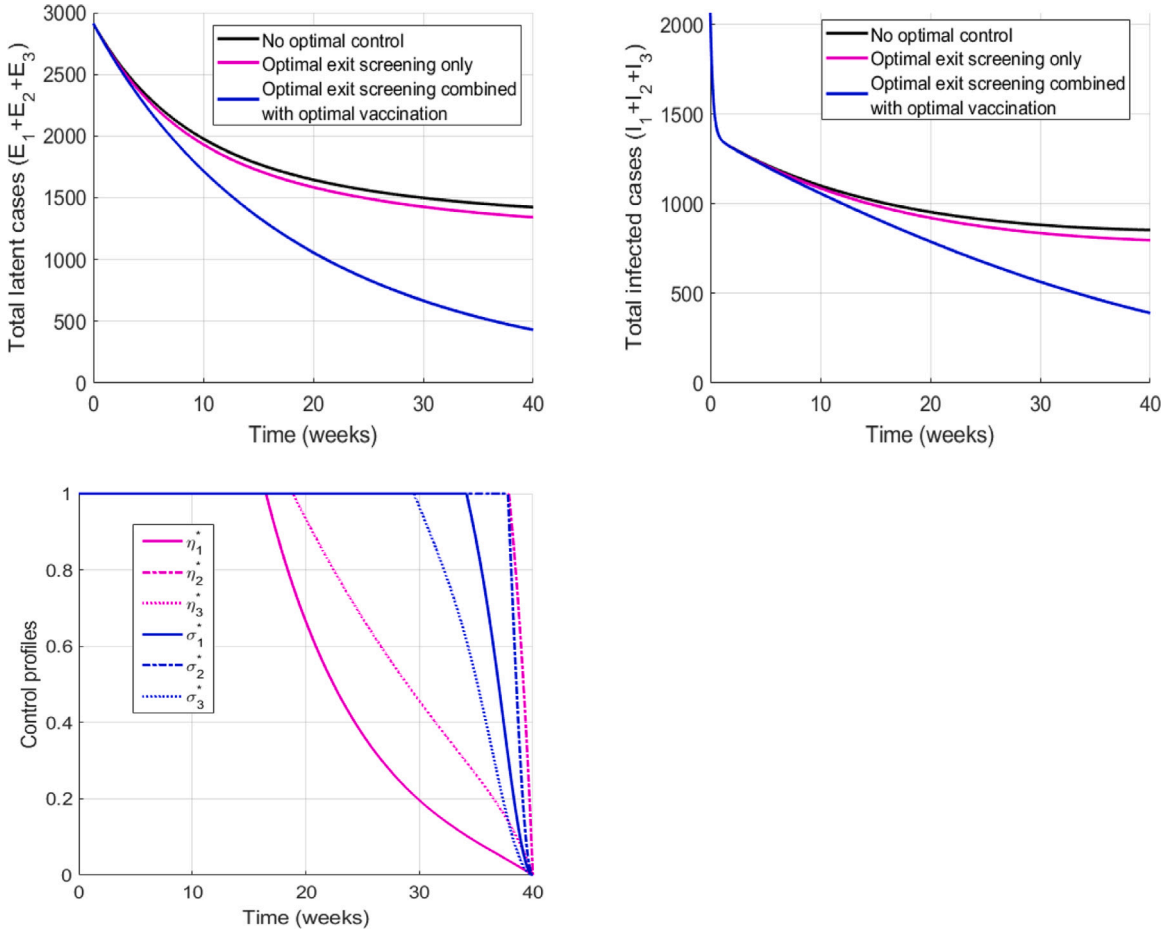


Fig. 6. Optimal control problem with exit screening combined or not combined with vaccination and solved with the NSFD scheme with $q = 500$, $h = 1$ for state variable and $h = 0.005$ for the adjoint variables. The values of the parameters are in Table 5.

We considered the optimal control problem for the well-known MSEIR model applied to the recent Measles outbreak in South Africa, with the vaccination as a control intervention [14,22]. Furthermore, using the exit screening of travellers [44] and the vaccination of susceptible individuals, we developed for the 2014–2016 EVD an extended SEIRD metapopulation model modified by additional compartments of quarantined and isolated individuals.

After investigating the dynamics (e.g. positivity and boundedness of solutions, stability of equilibria, etc.) of the state variable systems, we designed Euler-based NSFD versions of the forward–backward-sweep method (NSFD-FBSM) that preserve the dynamics of the state variable systems. We generated numerical simulations that support the theory and highlight the superiority of the NSFD-FBSM over the classical FBSM in the sense that the classical FBSM leads to negative solutions and does not highlight the impact of the control measures implemented. The nonstandard-based numerical simulations suggest that significantly increasing the coverage of the MMR vaccine with its implementation for adults as well, is vital and essential to stop the recurrent measles outbreaks in South Africa, a finding that aligns with [29]. Likewise, our simulations show that the optimal vaccination control for the 2014–2016 West Africa Ebola Virus Disease is more efficient to mitigate the number of infected individuals than the exit screening intervention.

Though being a more efficient intervention, the vaccination is modelled in this work in the simplest manner by assuming that it is 100% effective, which is not always the case. We plan to address this concern by adding a separate compartment that accounts for vaccinated individuals who then are infected at a reduced rate [45]. Moreover, since the Euler-based scheme are of order 1, this work can be extended by considering higher-order NSFD schemes such as the (modified) theta, the Runge–Kutta and the time-reversible methods developed in [5,32,46–48], respectively. In the patch model, we did not considered the residence place of individuals [49]. This aspect can be investigated with possibly additional control parameters of treatment such as the recently approved Ebanga drug [50].

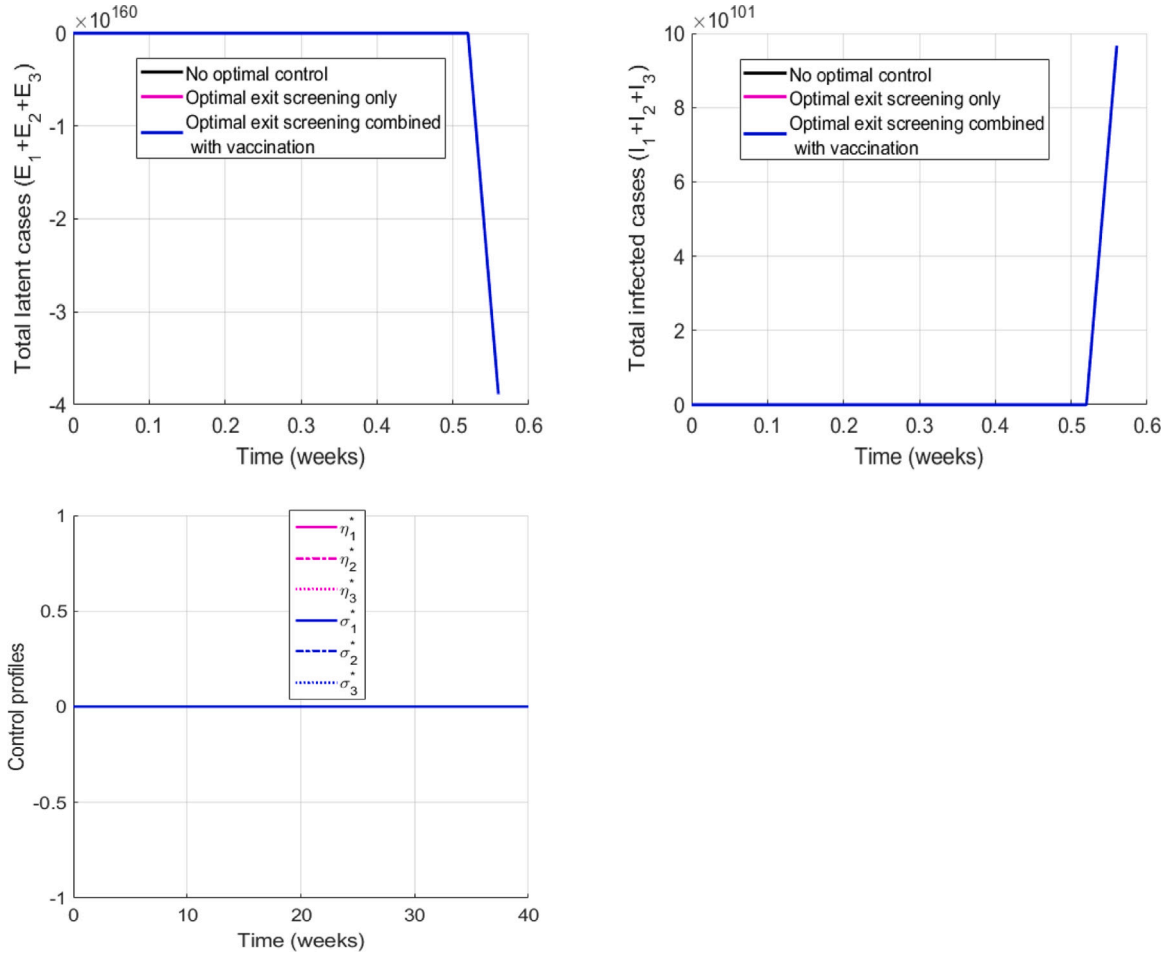


Fig. 7. Optimal exit screening combined or not with vaccination solved with the classical Euler FBSM with $h = 0.05$ for the state and adjoint variables. The values of the parameters are in Table 5. The dynamical inconsistency of the classical scheme with respect to the impact of the control measure is apparent.

CRediT authorship contribution statement

Arsène J. Ouemba Tassé: Writing – review & editing, Writing – original draft, Resources, Project administration, Methodology, Formal analysis, Data curation, Conceptualization. **Vuyiswa B. Kubalasa:** Writing – original draft, Resources, Conceptualization. **Berge Tsanou:** Writing – review & editing, Supervision, Methodology, Conceptualization. **Jean M.-S Lubuma:** Writing – review & editing, Writing – original draft, Supervision, Resources, Project administration, Methodology, Funding acquisition, Formal analysis, Conceptualization.

Declaration of competing interest

The authors declare that they have no known competing financial interests or personal relationships that could have appeared to influence the work reported in this paper.

Acknowledgements

The authors would like to thank Professor Rosa Maria Spitaleri, President of the International Association for Mathematics and Computers in Simulation (IMACS), for her kind invitation to present the material of this work at the 21st IMACS World Congress, 11–15 September 2023. They also thank the anonymous reviewers for suggesting the incorporation of new perspectives that have improved the paper. J.M.-S. Lubuma and A.J. Ouemba Tassé acknowledge the support of the National Research Foundation (NRF) under the Competitive Programme for Rated Researchers (CPRR: Grant no. 138013). They also acknowledge the support of the University of the Witwatersrand under the Science Faculty Start-up Funds for Research and the Postdoctoral Programme. B. Tsanou acknowledges the hospitality of the University of the Witwatersrand where this work was finalized during his research visit.

References

[1] R.E. Mickens, Difference equation models having zero local truncation errors, in: I.W. Knowles, R.T. Lewis (Eds.), Differential Equations, North-Holland, Amsterdam, 1984, pp. 445–449.
[2] Mickens R.E., Exact solutions to difference equation models of Burgers' equation, Numer. Methods Partial Differential Equations 2 (1986) 123–129.
[3] R.E. Mickens, Nonstandard Finite Difference Models of Differential Equations, World Scientific, Singapore, 1994.
[4] R.E. Mickens, Applications to Nonstandard Finite Difference Scheme, World Scientific, Clark Atlanta University, Atlanta, Georgia, 2000.
[5] F.K. Alalhareth, M. Gupta, S. Roy, H.V. Kojouharov, Second-order modified positive and Elementary Stable Nonstandard Numerical Methods for n-dimensional autonomous differential equations, Math. Methods Appl. Sci. (2023) 1–21, (Alalharethetal.).
[6] R. Anguelov, T. Berge, M. Chapwanya, J.K. Djoko, P. Kama, J.M.-S. Lubuma, Y. Terefe, Nonstandard finite difference method revisited and application to the Ebola virus disease transmission dynamics, J. Difference Equ. Appl. 26 (6) (2020) 818–854.
[7] R. Anguelov, J.M-S. Lubuma, Contributions to the mathematics of the nonstandard finite difference methods and applications, Numer. Methods Partial Differential Equations 17 (5) (2001) 518–543.
[8] M. Chapwanya, J. Lubuma, Y. Terefe, B. Tsanou, Analysis of war and conflict effect on the transmission dynamics of the tenth Ebola outbreak in the democratic Republic of Congo, Bull. Math. Biol. 84 (136) (2022) 1–48.
[9] D.T. Dimitrov, H.V. Kojouharov, B.M. Chen-Charpentier, Reliable Finite Difference Schemes with Applications in Mathematical Biology, Mickens, R.E., in: Advances in the Applications of Nonstandard Finite Difference Schemes, World Scientific, Singapore, 2005, pp. 249–285.
[10] R.E. Mickens, Nonstandard Finite Difference Schemes: Methodology and Applications, World Scientific, Singapore, 2020.
[11] A.B. Gumel, J. Difference Equ. Appl. 9 (2003) Guest-Ed (special issue).
[12] R. Mickens (Ed.), Advances in the Applications of Nonstandard Finite Difference Schemes, World Scientific, Singapore, 2005.
[13] Patidar K.C., Nonstandard finite difference methods: Recent trends and further developments, J. Difference Equ. Appl. 22 (6) (2016) 817–849.
[14] H.W. Hethcote, The mathematics of infectious diseases, SIAM Rev. 42 (2000) 599–653.
[15] S.A. Somma, N.I. Akinwande, Sensitivity analysis for the mathematical modeling of measles disease incorporating temporary passive immunity, in: Proceedings of 1st SPS Biennial International Conference Federal University of Technology, Minna, 2017, (Sommaetal.).
[16] T. Berge, A.J. Ouemba Tassé, H.M. Tenkam, J. Lubuma, Mathematical modeling of contact tracing as a control strategy of Ebola Virus Disease, Int. J. Biomath. 11 (2018) 1850093–1–36.
[17] OAG, Ebola statistics: For the most up-to-date information regarding the Ebola crisis please see our commentary below, 2023, (EbolaStatistics). Last access 03 May 2023.
[18] Unicef, Guinea migration profiles, 2013, (Guineapopulation). Last access 26-April-2023.
[19] Unicef, Liberia migration profiles, 2013, Last access 26-April-2023.
[20] Unicef, Sierra leone migration profiles, 2013, (SierraLeonePopulation). Last access 26-April-2023.
[21] V.B. Kubalasa, On Infectious Disease Transmissions and Optimal Control By Pontryagin's Maximum Principle, University of the Witwatersrand Johannesburg, 2022, Honours Project.
[22] S. Lenhart, J.T. Workman, Optimal Control Applied to Biological Models, Mathematical and Computational Biology Series, Chapman & Hall/CRM, New York, 2007.
[23] A.C. Chiang, Elements of Dynamic Optimization, McGrow-Hill International Editions, New York, 1999.
[24] M. McAsey, L. Mou, W. Han, Convergence of the forward-backward sweep method in optimal control, Comput. Optim. Appl. 53 (1) (2012) 207–226.
[25] H.R. Thieme, Mathematics in Population Biology, Princeton University Press, Princeton, 2003.
[26] National Institute for Communicable Diseases, South Africa measles outbreak update 2023, 2023, (MeaslesSouthAfricaCases). Last access 12-01-2024.
[27] Z. Shuai, P. Van den Driessche, Global stability of infections disease models using Lyapunov functions, SIAM J. Appl. Math. 73 (2013) 1513–1532.
[28] A. Bailey, A. Sapra, MMR Vaccine, National Library of Medicine, 2022, (MMRvaccine). Last access 28 December 2023.
[29] M.O. Oduoye, V. Zuhair, A. Marbell, G.D. Olatunji, A.A. Khan, A. Farooq, A.T. Jamiu, K.A. Karim, The recent meales outbreak in South Africa region is due to low vaccination coverage. What should we do to mitigate it? New Microbes New Infect. 54 (2023) (Oduoyeetal.).
[30] J.N.C. Gonçalves, Epidemiological Models and Optimal Control Theory - Applications To Marketing and Computer Viruses Transmission (Ph.D. thesis), Universidade do Minho, 2017.
[31] C.M. Baker, P. Blonda, F. Casella, F. Diele, C. Marangi, et al., Optimal spatiotemporal model for invasive plant management: the case of ailanthus altissima in the alta murgia national park (supplementary information), Sci. Rep. 13 (2023) 14587, (Sympleticscheme).
[32] R. Anguelov, Y. Dumont, J. Lubuma, M. Shillor, Dynamically consistent nonstandard finite difference schemes for epidemilogical models, J. Comput. Appl. Math. 255 (2013) 161–182.
[33] A.J. Ouemba Tassé, B. Tsanou, J.L. Woukeng, J. Lubuma, Metapopulation models with entry-exit screening and vaccination measures for the 2014–2016 West Africa Ebola virus outbreak, 2024, Under review.
[34] CDC, Ebola vaccine: Information about ERVEBO, 2023, (Ebolavaccine). Last access 27-10-2023.
[35] S. Merler, M. Ajelli, L. Fumanelli, S. Parlamento, A.P.Y. Piontti, N.E. Dean, G. Putoto, D. Carraro, I.M. Longini, J.M.E. Halloran, A. Vespignani, Containing Ebola at the source with ring vaccination, PLoS Negl. Trop. Dis. 10 (11) (2016) 1–11.
[36] A. Camacho, R.M. Eggo, S. Funk, C.H. Watson, Kucharski, W.J. Edmonds, Estimating the probability of demonstrating vaccine efficacy in the declining Ebola epidemic: a Bayesian modelling approach, BMJ Open 5 (2015) e009346, 1–6.
[37] C.M. Rivers, E.T. Lofgren, M. Marathe, S. Eubank, B.L. Lewis, Modelling the impact of interventions on an epidemic of Ebola in Sierra Leone and Liberia, PLOS Curr. Outbreaks (2014) (ImpactoftheinterventionsinSierraLeone).
[38] F.B. Agusto, M.I. Teboh-Ewungkem, A.B. Gumel, Mathematical assessment of the effect of traditional beliefs and customs on the transmission dynamics of the 2014 Ebola outbreaks, BMC Med. 13 (96) (2015) 1–17.
[39] T.W. Tulu, B. Tian, Z. Wu, Modeling the effect of quarantine and vaccination on Ebola disease, Adv. Difference Equ. 178 (2017) 1–14.
[40] Z.-Q. Xia, S.-F. Wang, S.-L. Li, L.-Y. Huang, W.-Y. Zhang, G.-Q. Sun, Z.-T. Gai, Z. Jin, Modeling the transmission dynamics of Ebola virus disease in Liberia, Sci. Rep. 5 (2015) 13857.
[41] E. Grigorieva, E. Khailov, Determination of the optimal controls for an Ebola epidemic model, Discrete Continuous Dyn. Syst. Ser. B 11 (2018) 1071–1101.
[42] Rachab A., A mathematical model with isolation for the dynamics of Ebola virus, 3rd international conference on mathematical sciences and statistics, J. Phys. Conf. Ser. 1132 (2018) (Rachabatthe3rdConference).
[43] A.J. Ouemba Tassé, B. Tsanou, J. Lubuma, J.L. Woukeng, F. Signing, Ebola virus disease dynamics with some preventive measures: a case study of the 2018–2020 Kivu outbreak, J. Biol. Syst. 30 (2022) 113–148.
[44] WHO, Interim guidance for Ebola virus disase: Exit screening at airports, ports and land crossings, 2014, 1–25, (ExitScreeningGuidance).
[45] S. Liao, W. Yang, On the dynamics of a vaccination model with multiple transmission ways, Int. J. Appl. Math. Comput. Sci. 22 (2013) 761–772.
[46] Q.A. Dang, M.T. Hoang, Positive and elementary stable explicit nonstandard Runge–Kutta methods for a class of autonomous dynamical systems, Int. J. Comput. Math. 97 (10) (2020) 2036–2054, (NSFD-Runge--Kutta).
[47] R. Anguelov, J.M-S. Lubuma, Forward invariant set preservation in discrete dynamical systems and numerical schemes for ODEs: Application in biosciences, Adv. Contin. Discrete Models: Theory Modern Appl. 2023 (2023) 38, (ForwardInvariantsetPreservation).

[48] R. Anguelov, J.M-S. Lubuma, A second order nonstandard finite difference scheme and application to model of biological and chemical processes, in: A. Gumel (Ed.), Mathematical and Computational Modeling of Phenomena Arising in Population Biology and Nonlinear Oscillations (Volume in Honour of Ronald E. Mickens 80th Birthday), in: Contemporary Mathematics, vol. 793, American Mathematical Society, 2024, pp. 1–15, (ASecondOrderNSFDSchemeandApplications).

[49] B. Espinoza, V. Moreno, D. Bichara, C. Castillo-Chavez, Assessing the efficiency of movement restriction as a control strategy of Ebola, Math. Stat. Model. Emerg. Re-Emerg. Infect. Dis. (2016) 123–145, (MovementrestrictionagainstEbola).

[50] E. Taki, R. Ghanavati, T. Navidifar, S. Dashtbin, M. Heidary, M. Moghadamnia, Ebanga: The most recent FDA-approved drug for treating Ebola, Front. Pharmacol. 14 (2023) 1083429, (Ebolatreatment).